

Spring School on Superconducting Qubit Technology

2023/4/19, 9:30-11:00

Centro de Ciencias de Benasque Pedro Pascual

Physics and Applications of Kerr Parametric Oscillators

¹Secure System Platform Research Laboratories, NEC Corporation

²NEC-AIST Quantum Technology Cooperative Research Laboratory, The National Institute of Advanced Industrial Science and Technology

Tsuyoshi Yamamoto

Slide courtesy

Table of Contents

1. Brief overview
2. Introduction of KPO
 - theoretical description
3. Application of KPO in FTQC
4. Application of KPO in quantum annealing
5. Summary



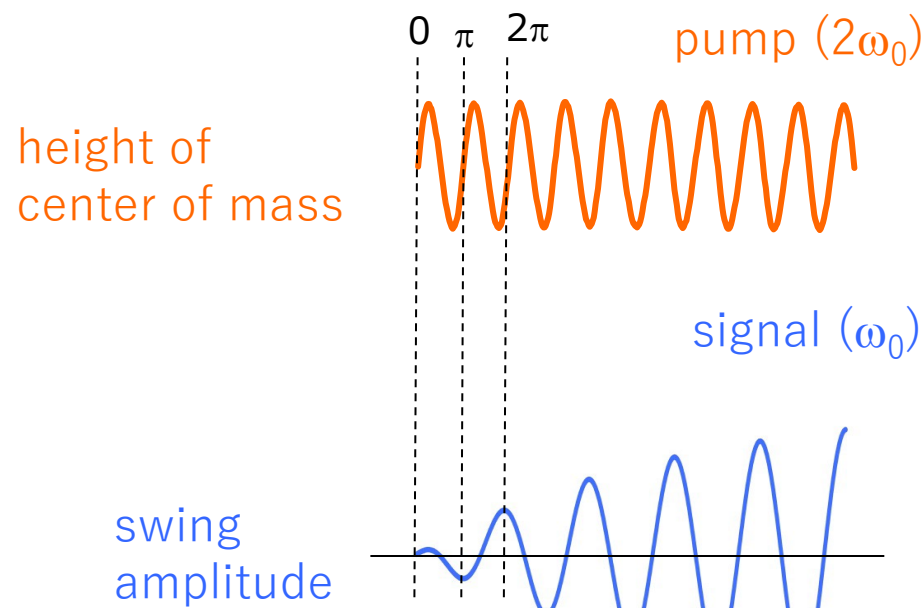
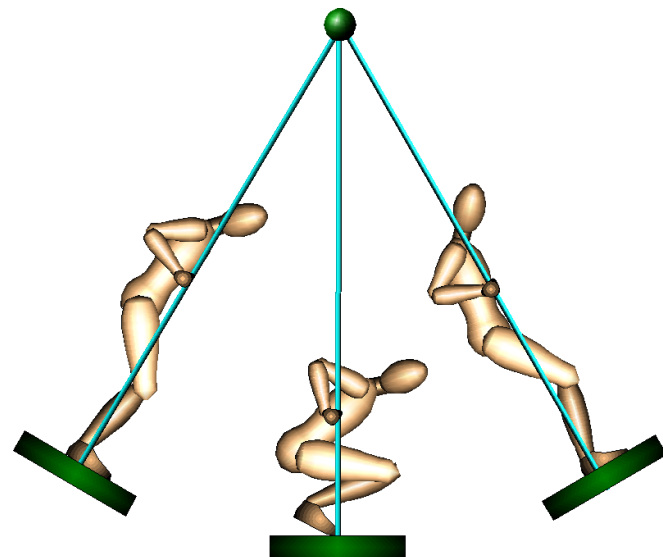
Shumpei Masuda Ryoji Miyazaki

Table of Contents

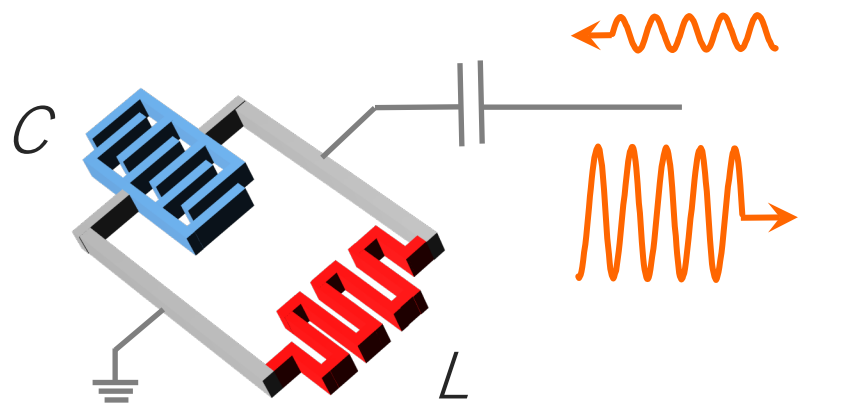
1. Brief overview
2. Introduction of KPO
 - theoretical description
3. Application of KPO in FTQC
4. Application of KPO in quantum annealing
5. Summary

Parametric resonance

- ◆ Modulation of a parameter of an oscillating system at twice the resonant frequency leads to the amplification of the oscillation.



Parametric amplifier



$$\omega_0 = \frac{1}{\sqrt{LC}}$$

amplification!

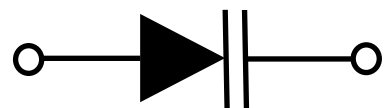


$$C + \delta C \cos 2\omega_0 t$$

OR



$$L + \delta L \cos 2\omega_0 t$$

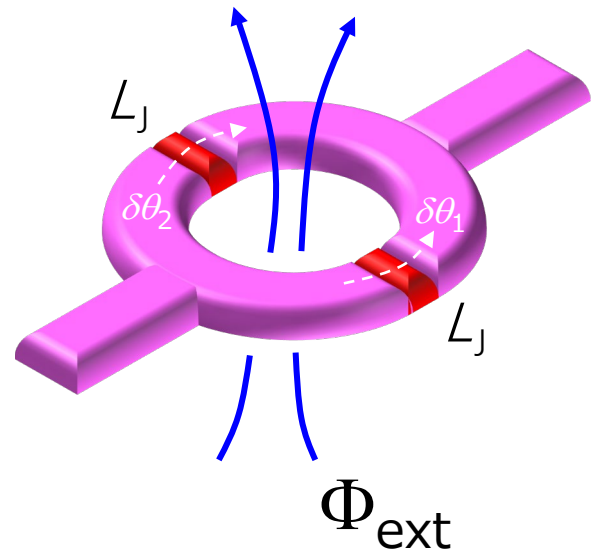


varactor diode



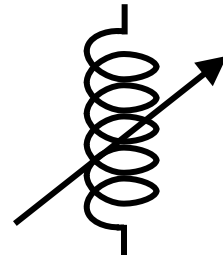
Josephson junction

Superconducting QUantum Interference Device (SQUID)



=

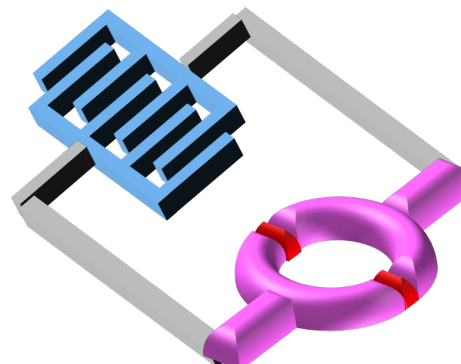
flux-tunable (nonlinear) inductor



$$L_J^{\text{eff}}(\Phi_{\text{ext}}) = \frac{L_J}{2} \frac{1}{\cos(\pi\Phi_{\text{ext}}/\Phi_0)}$$

Flux quantization:

$$\delta\theta_1 - \delta\theta_2 + 2\pi\Phi_{\text{ext}}/\Phi_0 = \text{integer}$$



$$\Phi_{\text{ext}}^0 + \delta\Phi \cos 2\omega_0 t$$

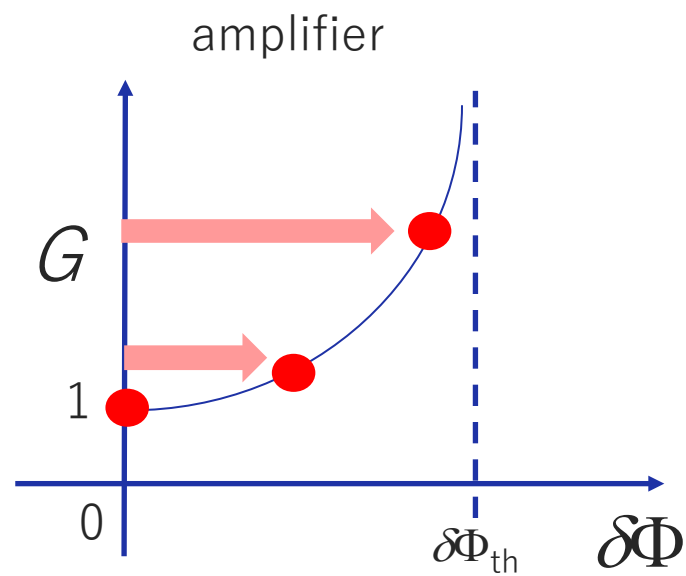
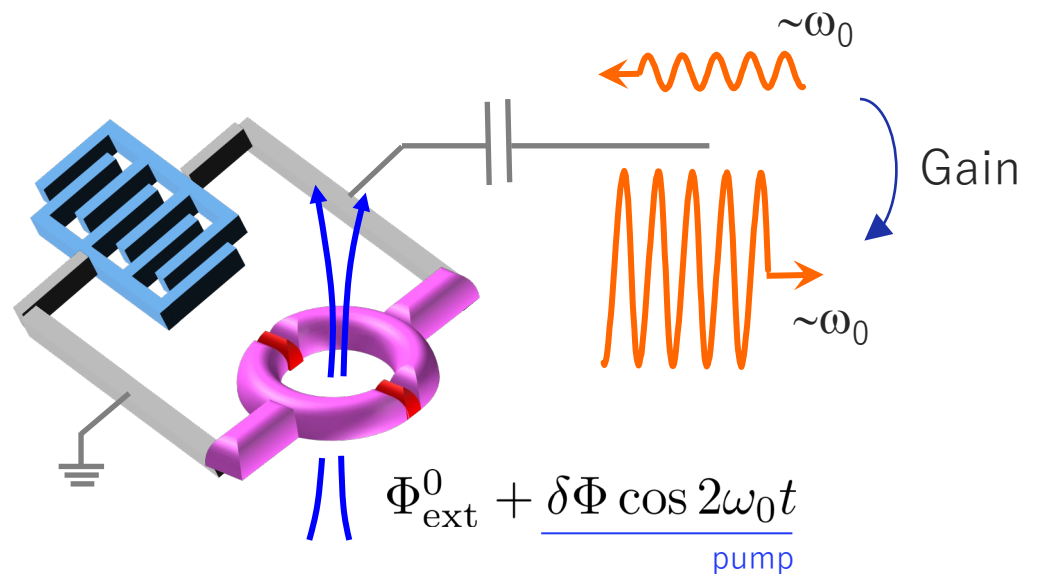
Flux-driven Josephson Parametric Amplifier (JPA)

T. Yamamoto *et al.*,
Appl. Phys. Lett. **93**, 042510 (2008).

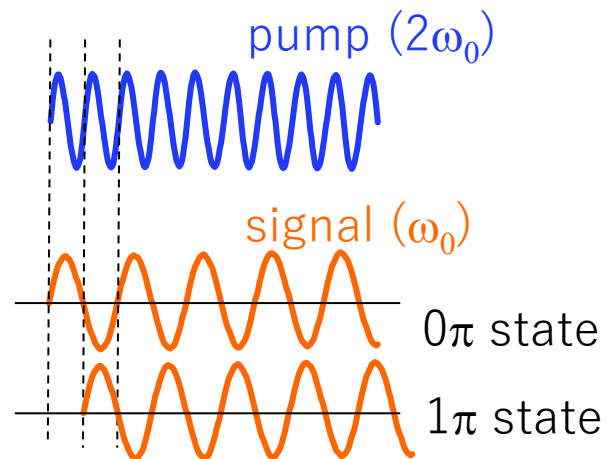
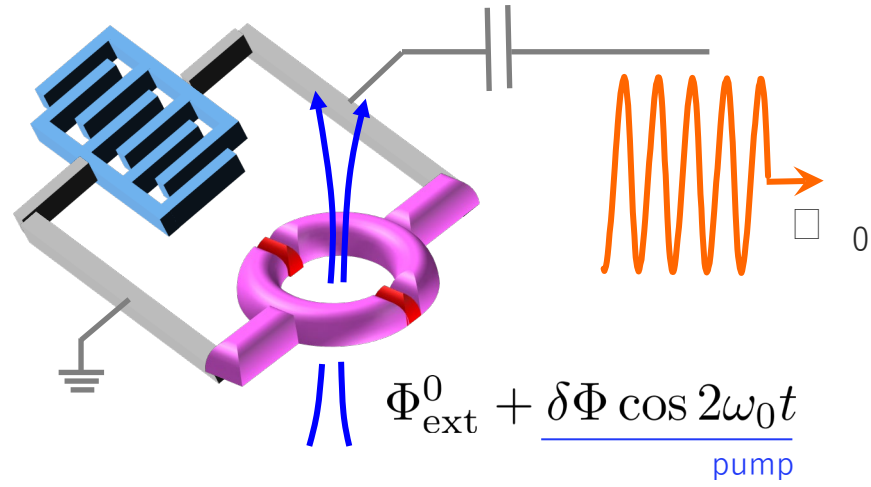
\Orchestrating a brighter world

NEC

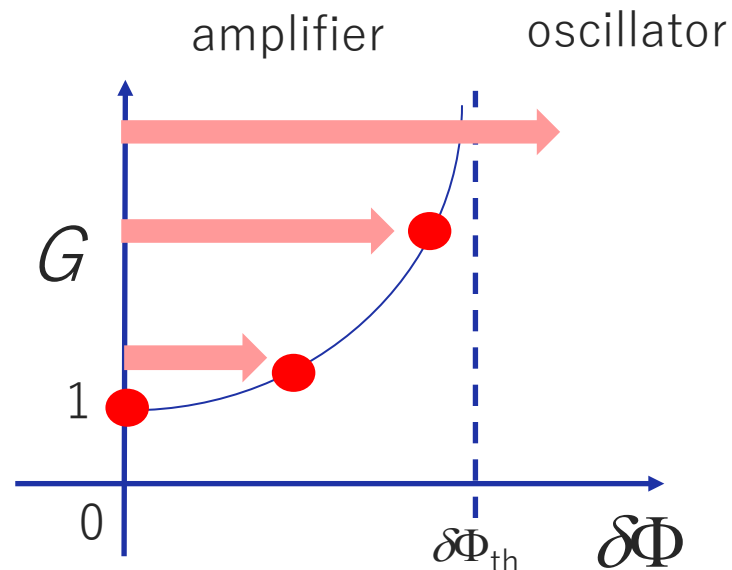
Josephson parametric oscillator



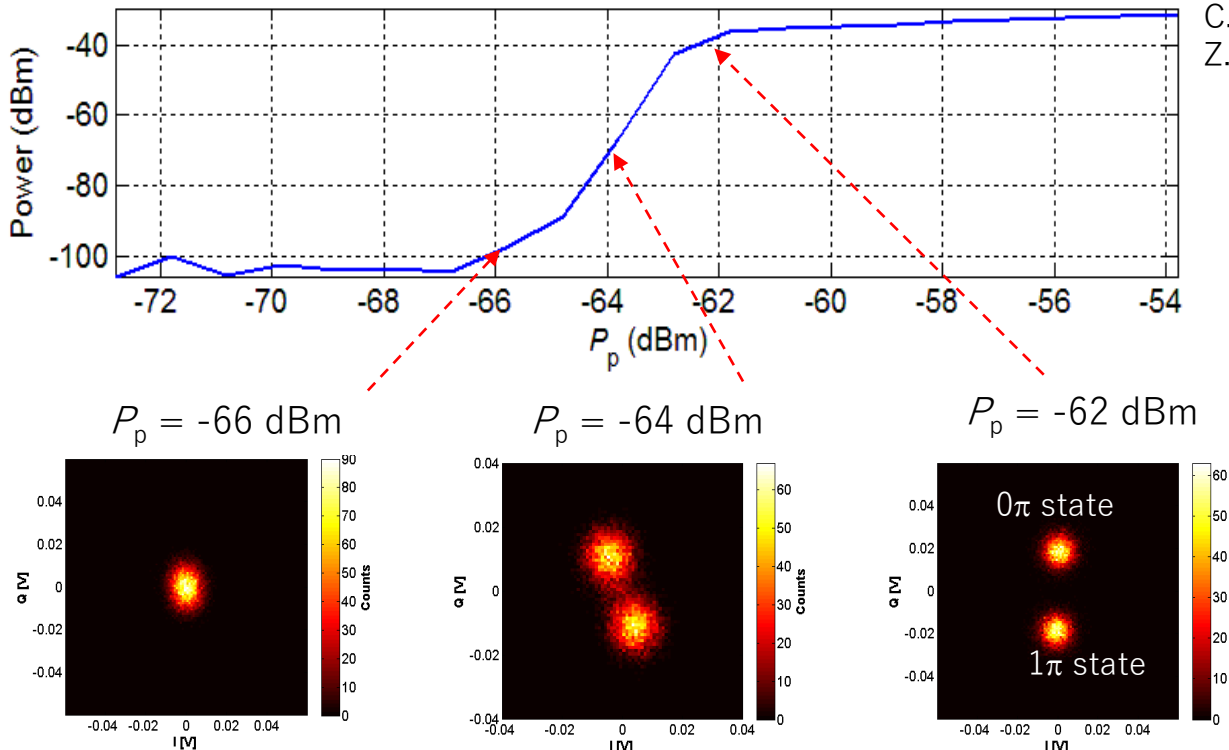
Josephson parametric oscillator



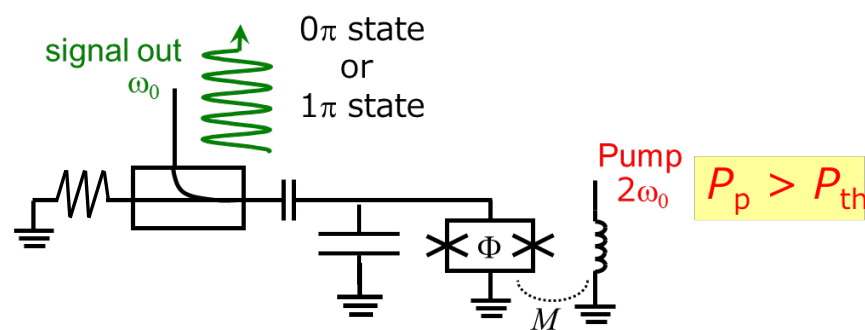
- 0π state and 1π state are generated randomly.
- Injecting external signal at ω_0 biases the probability.



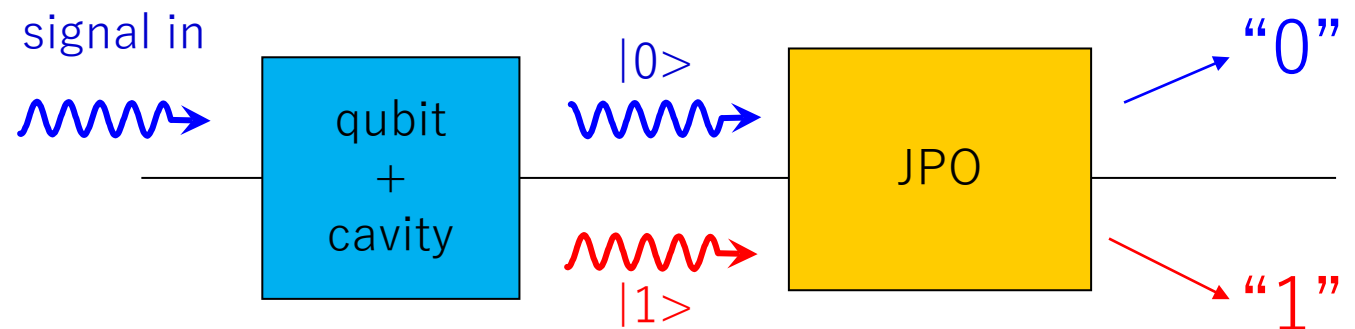
(Classical) Josephson parametric oscillator



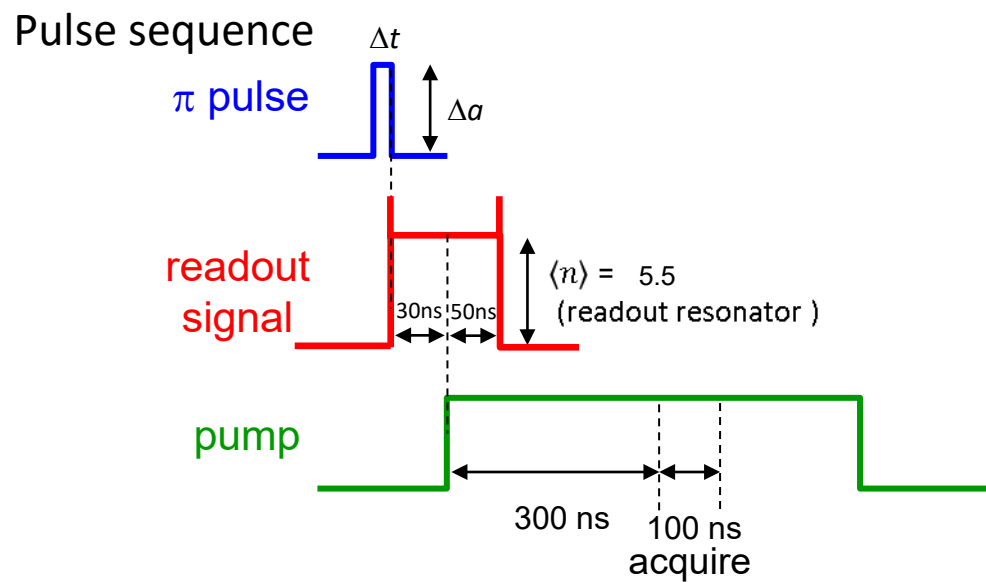
C. M. Wilson *et al.*, Phys. Rev. Lett. **105**, 233907 (2010).
Z. R. Lin *et al.*, Nature Commun. **5**, 4480 (2014).



qubit readout using JPO



Z. R. Lin *et al.*, Nature Commun. **5**, 4480 (2014).



Quantum annealing with JPO (theory)

Bifurcation-based adiabatic quantum computation with a nonlinear oscillator network

Hayato Goto

Sci. Rep. **6**, 21686 (2016).

SCIENCE ADVANCES | RESEARCH ARTICLE Sci. Adv. **3**, e1602273 (2017).

QUANTUM INFORMATION

Robust quantum optimizer with full connectivity

Simon E. Nigg,* Niels Lörch, Rakesh P. Tiwari

ARTICLE

Received 1 Nov 2016 | Accepted 28 Apr 2017 | Published 8 Jun 2017

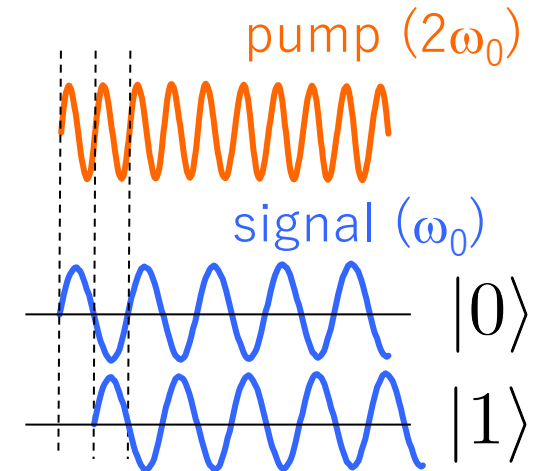
DOI: 10.1038/ncomms15785

OPEN

Quantum annealing with all-to-all connected nonlinear oscillators

Nature Commun. **8**, 15785 (2017).

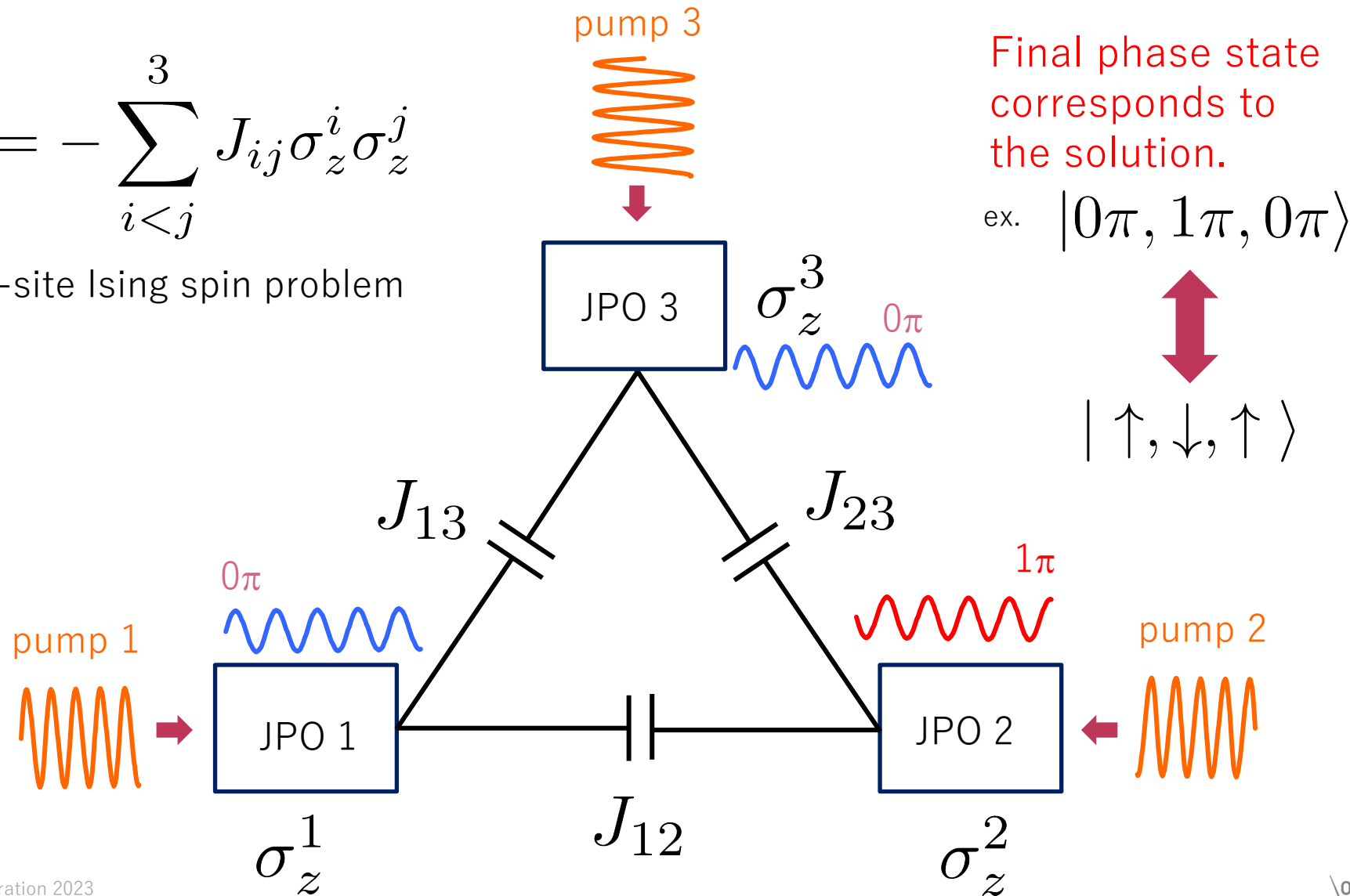
Shruti Puri¹, Christian Kraglund Andersen², Arne L. Grimsmo¹ & Alexandre Blais^{1,3}



Quantum annealing with JPO (intuitive)

$$\mathcal{H} = - \sum_{i < j}^3 J_{ij} \sigma_z^i \sigma_z^j$$

3-site Ising spin problem



Recent theories on JPO (KPO) annealing

- ◆ Boltzmann sampling
 - H. Goto et al., Sci. Rep. **8**, 7154 (2018).
- ◆ 3D cQED implementation
 - P. Zhao et al., Phys. Rev. Appl. **10**, 024019 (2018).
- ◆ Quantum annealing started with stable excited state
 - H. Goto and T. Kanao, Commun. Phys. **3**, 235 (2020).
- ◆ Comparison between quantum and classical models
 - M. J. Kewming et al., New J. Phys. **22**, 053042 (2020).
- ◆ All-to-all coupling via Floquet engineering
 - T. Onodera et al., npj Quantum Info. **6**, 48 (2020).
- ◆ Photon-number inhomogeneity and its mitigation in LHZ architecture
 - T. Kanao and H. Goto, npj Quantum Info. **7**, 1 (2021).
- ◆ Effective spin model of (bosonic) KPO
 - R. Miyazaki, Phys. Rev. A **105**, 062457 (2022).
- ◆ Controllable coupling between KPOs
 - S. Masuda et al., Phys. Rev. Appl. **18**, 034076 (2022).
- ◆ Effect of Nonstoquastic catalyst
 - Y. Susa et al., arXiv:2209.01737.

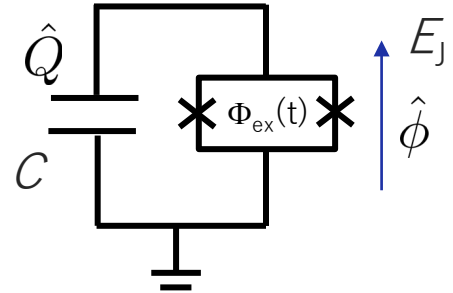
Proposals for hardware-efficient FTQC using Kerr cat qubit

- ◆ Theory of Kerr cat qubit
 - P. T. Cochrane et al., Phys. Rev. A **59**, 2631 (1999).
 - H. Goto, Phys. Rev. A **93**, 050301 (2016).
 - S. Puri et al., npj Quantum Info. **3**, 18 (2017).
- ◆ High-fidelity gate operation
 - T. Kanao et al., Phys. Rev. Appl. **18**, 014019 (2022).
 - H. Chono et al., Phys. Rev. Res. **4**, 043054 (2022).
- ◆ Proposal of bias preserving gate
 - S. Puri et al., Sci. Adv. 6, eaay5901 (2020).
- ◆ Error-correction code with high error threshold
 - A. S. Darmawan et al., PRX Quantum 2, 030345 (2021).

Table of Contents

1. Brief overview
2. Introduction of KPO
 - theoretical description
3. Application of KPO in FTQC
4. Application of KPO in quantum annealing
5. Summary

Hamiltonian of KPO



$$\begin{aligned}\mathcal{H}_{\text{KPO}} &= \frac{\hat{Q}^2}{2C} - E_J(t) \cos \hat{\phi} \\ &\simeq \frac{\hat{Q}^2}{2C} - E_J(t) \left(1 - \frac{1}{2} \hat{\phi}^2 + \frac{1}{24} \hat{\phi}^4\right)\end{aligned}$$

$$E_J(t) = E_J + \delta E_J \cos \omega_p t$$

$$\begin{aligned}\hbar\omega_0 &= \sqrt{8E_c E_J} \\ E_c &= e^2/2C\end{aligned}$$

$$\begin{aligned}\hat{\phi} &= \left(\frac{2E_c}{E_J}\right)^{1/4} (a^\dagger + a) \\ \hat{Q} &= i \left(\frac{E_J}{2E_c}\right)^{1/4} (a^\dagger - a)\end{aligned}$$

$$\mathcal{H}_{\text{KPO}} \simeq \hbar\omega_0 \left(a^\dagger a + \frac{1}{2}\right) - \frac{E_c}{12} (a^\dagger + a)^4 + \frac{\hbar\omega_0}{4} \frac{\delta E_J}{E_J} (a^\dagger + a)^2 \cos \omega_p t$$

Hamiltonian of KPO

$$\mathcal{H}_{\text{KPO}} = \hbar\omega_0 \left(a^\dagger a + \frac{1}{2} \right) - \frac{E_c}{12} (a^\dagger + a)^4 + \frac{\hbar\omega_0}{4} \frac{\delta E_J}{E_J} (a^\dagger + a)^2 \cos \omega_p t$$



rotating frame at $\omega_p/2$, and RWA

$$\mathcal{H}_{\text{KPO}}'/\hbar = \Delta a^\dagger a - \frac{K}{2} a^\dagger a^\dagger a a + \frac{\beta}{2} (a^\dagger{}^2 + a^2)$$

detuning Kerr nonlinearity parametric drive

$$\Delta = \omega_0 - K - \omega_p/2$$

$$K = E_c$$

$$\beta = \frac{\omega_0}{4} \frac{\delta E_J}{E_J}$$

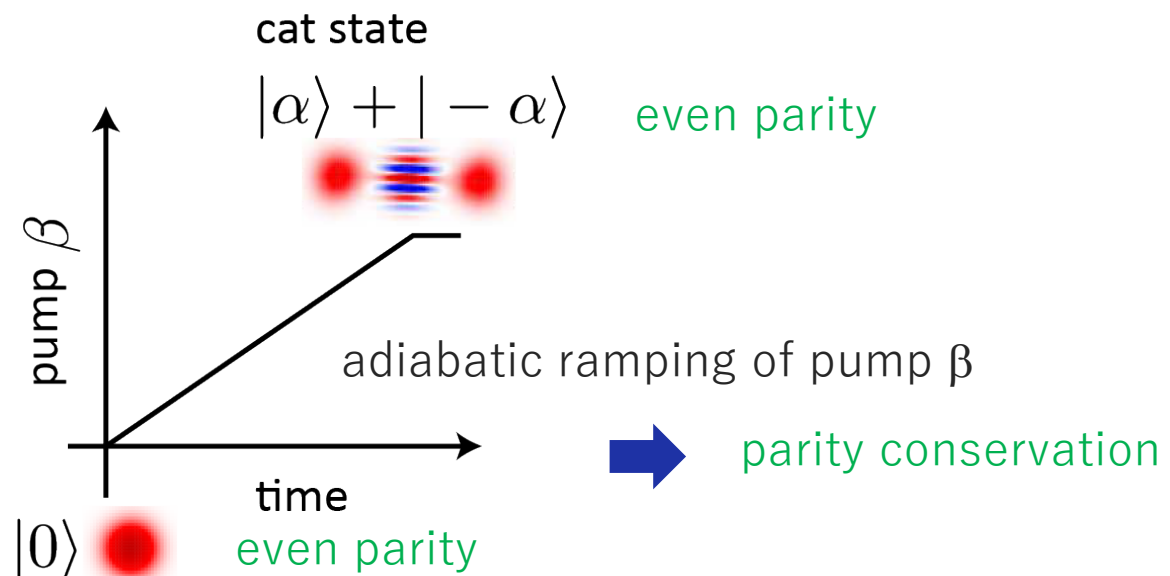
Generation of Schrodinger's cat state

$$\begin{aligned}\mathcal{H}_{\text{KPO}}/\hbar &= -\frac{K}{2}a^\dagger a^\dagger aa + \frac{\beta}{2}(a^{\dagger 2} + a^2) \\ &= -K\left(a^{\dagger 2} - \frac{\beta}{K}\right)\left(a^2 - \frac{\beta}{K}\right) + \frac{\beta^2}{K}\end{aligned}$$

P. T. Cochrane et al., Phys. Rev. A **59**, 2631 (1999).
H. Goto, Sci. Rep. **6**, 21686 (2016).
S. Puri et al., npj Quantum Info. **3**, 18 (2017).

Coherent state is an eigenstate of annihilation operator a , $a|\alpha\rangle = \alpha|\alpha\rangle$

\mathcal{H}_{KPO} has degenerate eigenstates of $|\pm\alpha\rangle$, where $\alpha = \sqrt{\frac{\beta}{K}}$



pitchfork bifurcation

M. I. Dykman, Phys. Rev. E **57**, 5202 (1998).

$$\dot{x} = y[\Delta + p + K(x^2 + y^2)] = 0$$

$$\dot{y} = x[-\Delta + p - K(x^2 + y^2)] = 0$$

solid lines:
classically stable points

$$\rightarrow x = \pm \sqrt{(p - \Delta)/K}$$

Wigner function below and
above the threshold

$$H_1 = \hbar\Delta a^\dagger a + \hbar\frac{K}{2}a^{\dagger 2}a^2 - \hbar\frac{p}{2}(a^2 + a^{\dagger 2})$$

Schrodinger's cat state

H. Goto, Sci. Rep. **6**, 21686 (2016).
<https://www.nature.com/articles/srep21686>

Fig. 1

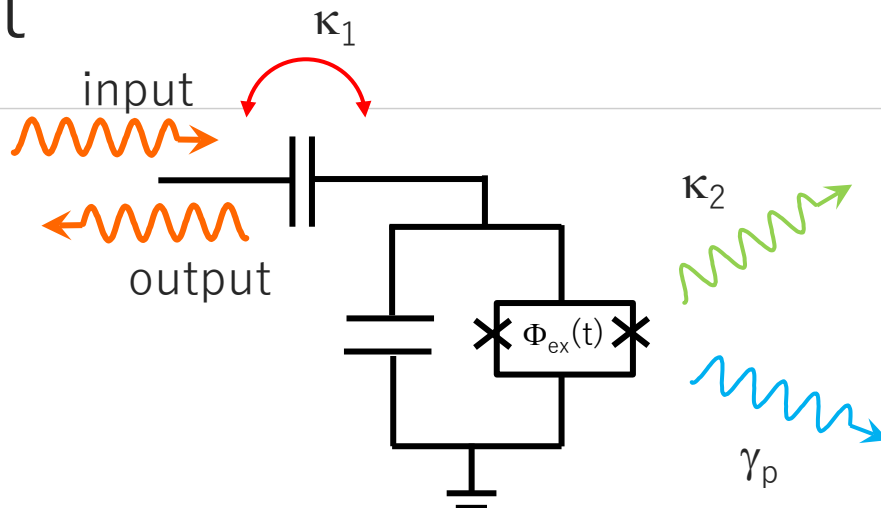
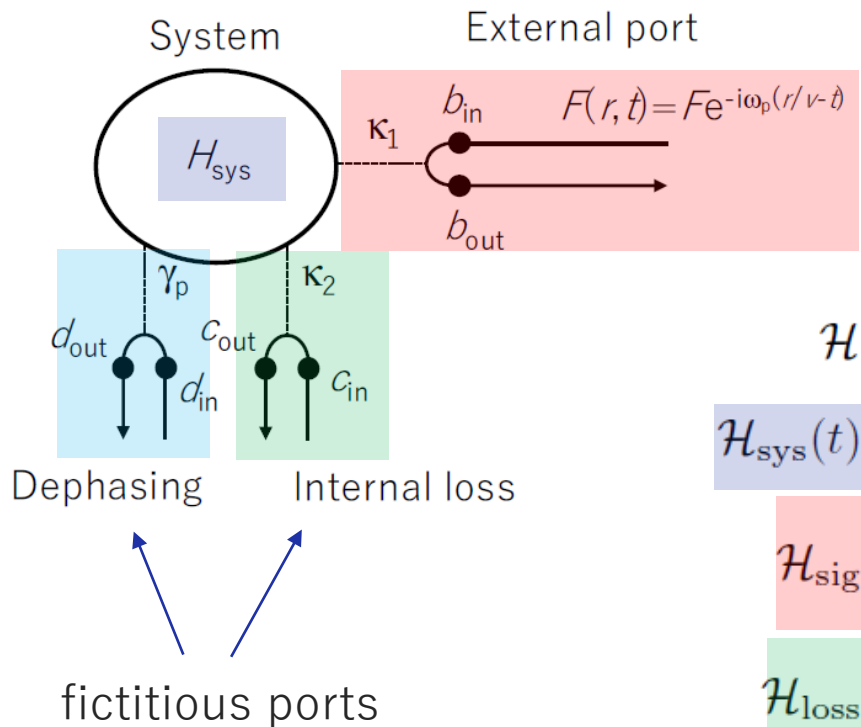


$$\frac{da}{dt} = \frac{i}{\hbar}[H_1, a]$$

$$a = x + iy$$

$$a^\dagger = x - iy$$

KPO coupled to environment



$$\mathcal{H}(t) = \mathcal{H}_{\text{sys}}(t) + \mathcal{H}_{\text{sig}} + \mathcal{H}_{\text{loss}} + \mathcal{H}_{\text{dep}},$$

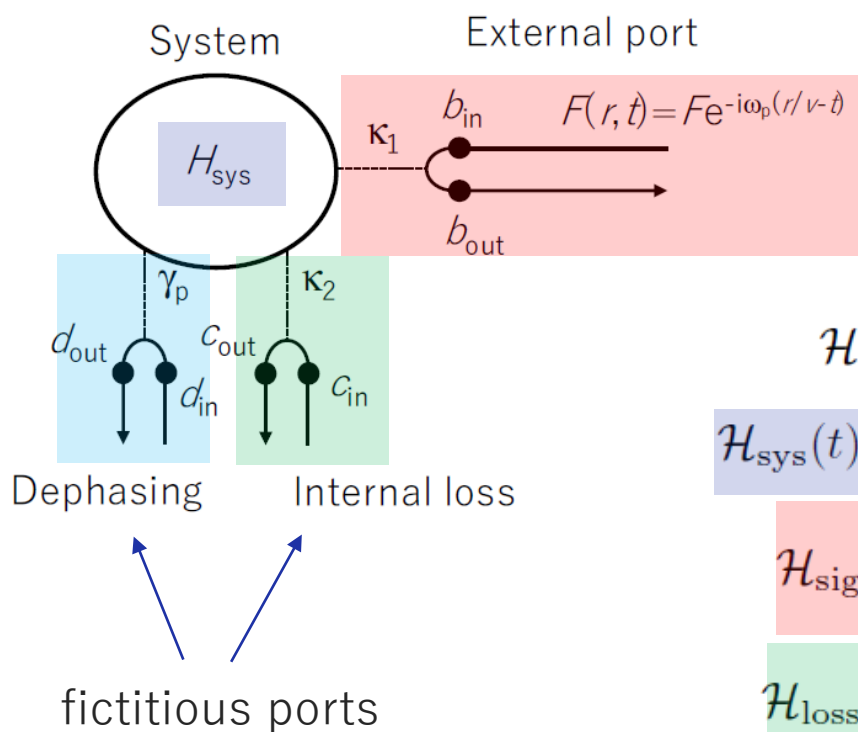
$$\mathcal{H}_{\text{sys}}(t)/\hbar = \Omega_0 a^\dagger a + \frac{K}{2} a^\dagger a^\dagger a a, \quad \text{w/o parametric drive}$$

$$\mathcal{H}_{\text{sig}}/\hbar = \int dk \left[v_b k b_k^\dagger b_k + \sqrt{\frac{v_b \kappa_1}{2\pi}} (a^\dagger b_k + b_k^\dagger a) \right],$$

$$\mathcal{H}_{\text{loss}}/\hbar = \int dk \left[v_c k c_k^\dagger c_k + \sqrt{\frac{v_c \kappa_2}{2\pi}} (a^\dagger c_k + c_k^\dagger a) \right],$$

$$\mathcal{H}_{\text{dep}}/\hbar = \int dk \left[v_d k d_k^\dagger d_k + \sqrt{\frac{v_d \gamma_p}{\pi}} a^\dagger a (d_k + d_k^\dagger) \right],$$

KPO coupled to environment



Input-output formalism

M. J. Collett and C. W. Gardiner,
Phys. Rev. A **30**, 1386 (1984).

$$b_{\text{in}}(t) \equiv \tilde{b}_{-0}(t) = \tilde{b}_{-vt}(0),$$

$$b_{\text{out}}(t) \equiv \tilde{b}_{+0}(t) = b_{\text{in}}(t) - i\sqrt{\frac{\kappa_1}{v}}a(t).$$

derived from Heisenberg's EOM for b_k

$$\mathcal{H}(t) = \mathcal{H}_{\text{sys}}(t) + \mathcal{H}_{\text{sig}} + \mathcal{H}_{\text{loss}} + \mathcal{H}_{\text{dep}},$$

$$\mathcal{H}_{\text{sys}}(t)/\hbar = \Omega_0 a^\dagger a + \frac{K}{2} a^\dagger a^\dagger a a, \quad \text{w/o parametric drive}$$

$$\mathcal{H}_{\text{sig}}/\hbar = \int dk \left[v_b k b_k^\dagger b_k + \sqrt{\frac{v_b \kappa_1}{2\pi}} (a^\dagger b_k + b_k^\dagger a) \right],$$

$$\mathcal{H}_{\text{loss}}/\hbar = \int dk \left[v_c k c_k^\dagger c_k + \sqrt{\frac{v_c \kappa_2}{2\pi}} (a^\dagger c_k + c_k^\dagger a) \right],$$

$$\mathcal{H}_{\text{dep}}/\hbar = \int dk \left[v_d k d_k^\dagger d_k + \sqrt{\frac{v_d \gamma_p}{\pi}} a^\dagger a (d_k + d_k^\dagger) \right],$$

Input-output formalism

- ◆ By solving Heisenberg's equation of motion for appropriate operator, e.g., a , $a^\dagger a$, and $|m\rangle\langle n|$, we can calculate various physical quantities such as reflection coefficient, fluorescence spectra, amplifier's gain.
- ◆ Example 1: Reflection coefficient

Heisenberg's equation of motion for a

$$b_{\text{out}}(t) \equiv \tilde{b}_{+0}(t) = b_{\text{in}}(t) - i\sqrt{\frac{\kappa_1}{v}}a(t).$$

$$\begin{aligned}\frac{da}{dt} &= i[\mathcal{H}(t)/\hbar, a] \\ &= i[\mathcal{H}_{\text{sys}}(t)/\hbar, a] - \frac{\kappa_1 + \kappa_2}{2}a + \gamma_p[a^\dagger a, a] \\ &\quad - i\sqrt{v\kappa_1}b_{\text{in}}(t) - i\sqrt{v\kappa_2}c_{\text{in}}(t) - i\sqrt{2v\gamma_p}[ad_{\text{in}}(t) + d_{\text{in}}^\dagger(t)a] \\ &= -\left(i\Omega_0 + iKa^\dagger a + \frac{\kappa}{2}\right)a - i\sqrt{v\kappa_1}b_{\text{in}}(t) - i\sqrt{v\kappa_2}c_{\text{in}}(t) - i\sqrt{2v\gamma_p}[ad_{\text{in}}(t) + d_{\text{in}}^\dagger(t)a]\end{aligned}$$

$$\kappa = \kappa_1 + \kappa_2 + 2\gamma_p$$

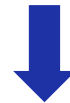
Reflection coefficient

Take the expectation value by initial state of the system and neglect the nonlinear term $\langle a^\dagger a a \rangle$ to consider weak probe power limit.

$$\frac{d\langle a \rangle}{dt} = -\left(i\Omega_0 + \frac{\kappa}{2}\right)\langle a \rangle$$

no signal on the fictitious ports

$$-i\sqrt{v\kappa_1}\langle b_{\text{in}}(t) \rangle - i\sqrt{v\kappa_2}\langle c_{\text{in}}(t) \rangle - i\sqrt{2v\gamma_p}[\langle ad_{\text{in}}(t) \rangle + \langle d_{\text{in}}^\dagger(t)a \rangle]$$



$$d/dt \rightarrow -i\omega_{\text{in}}$$

$$\langle a \rangle = \frac{-i\sqrt{v\kappa_1}}{-i(\omega_{\text{in}} - \Omega_0) + \kappa/2} \langle b_{\text{in}} \rangle$$

$$\langle b_{\text{out}} \rangle = \langle b_{\text{in}} \rangle - i\sqrt{\frac{\kappa_1}{v}}\langle a \rangle$$

reflection coefficient Γ

$$= \left[1 - \frac{\kappa_1}{-i(\omega_{\text{in}} - \Omega_0) + \kappa/2} \right] \langle b_{\text{in}} \rangle.$$

$$\kappa = \kappa_1 + \kappa_2 + 2\gamma_p$$

e.g. calculated Γ

over-coupled

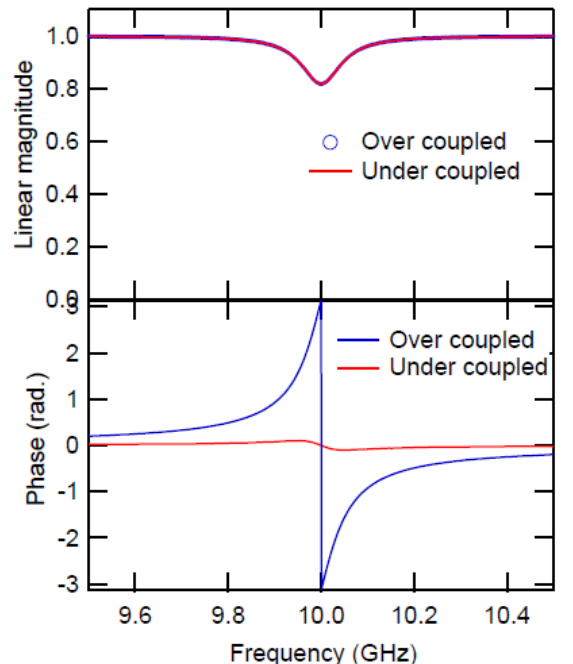
$$\kappa_1/2\pi = 100 \text{ MHz}$$

$$\kappa/2\pi = 110 \text{ MHz}$$

under-coupled

$$\kappa_1/2\pi = 10 \text{ MHz}$$

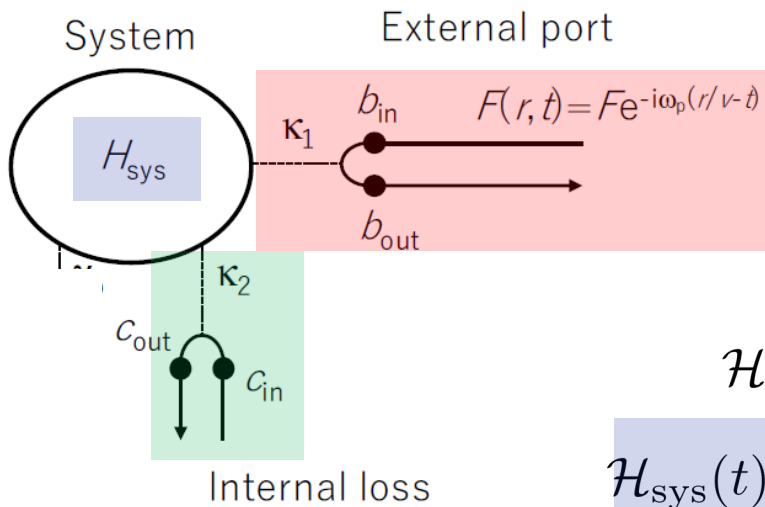
$$\kappa/2\pi = 110 \text{ MHz}$$



note: Γ does not tell κ_2 from γ_p .

Input-output formalism

◆ Example 2: Master equation



T. Yamamoto, in Springer Lecture Notes in Physics
"Quantum Computing, Quantum Communication and Quantum Metrology"
edited by Y. Yamamoto and K. Sembra

$$b_{\text{in}}(t) \equiv \tilde{b}_{-0}(t) = \tilde{b}_{-vt}(0),$$
$$b_{\text{out}}(t) \equiv \tilde{b}_{+0}(t) = b_{\text{in}}(t) - i\sqrt{\frac{\kappa_1}{v}}a(t).$$

derived from Heisenberg's EOM for b_k

$$\mathcal{H}(t) = \mathcal{H}_{\text{sys}}(t) + \mathcal{H}_{\text{sig}} + \mathcal{H}_{\text{loss}},$$
$$\mathcal{H}_{\text{sys}}(t)/\hbar = \Omega_0 a^\dagger a + \frac{K}{2} a^\dagger a^\dagger a a + \beta(a^\dagger + a)^2 \cos \omega_p t$$

$$\mathcal{H}_{\text{sig}}/\hbar = \int dk \left[v_b k b_k^\dagger b_k + \sqrt{\frac{v_b \kappa_1}{2\pi}} (a^\dagger b_k + b_k^\dagger a) \right]$$

$$\mathcal{H}_{\text{loss}}/\hbar = \int dk \left[v_c k c_k^\dagger c_k + \sqrt{\frac{v_c \kappa_2}{2\pi}} (a^\dagger c_k + c_k^\dagger a) \right]$$

forget about dephasing for the moment

Master equation

Heisenberg's equation of motion for $s_{mn}(t) \equiv |m\rangle\langle n|$

$$\frac{d}{dt}s_{mn}(t) = -i[s_{mn}(t), \mathcal{H}/\hbar]$$

Using

$$\left[s_{mn}, \frac{1}{\sqrt{2}} \int dk a^\dagger b_k \right] = [s_{mn}, a^\dagger] b_{\text{in}} + \frac{1}{2} \sqrt{\frac{\kappa_1}{v}} (a^\dagger s_{mn} a - s_{mn} a^\dagger a),$$

$$\left[s_{mn}, \frac{1}{\sqrt{2}} \int dk b_k^\dagger a \right] = b_{\text{in}}^\dagger [s_{mn}, a] - \frac{1}{2} \sqrt{\frac{\kappa_1}{v}} (a^\dagger s_{mn} a - a^\dagger a s_{mn})$$

$$\begin{aligned} \frac{d}{dt}s_{mn} &= \frac{-i}{\hbar}[s_{mn}, \mathcal{H}_{\text{sys}}(t)] + \frac{\kappa}{2}(2a^\dagger s_{mn} a - s_{mn} a^\dagger a - a^\dagger a s_{mn}) \\ &\quad + \sqrt{v\kappa_1}[s_{mn}, a^\dagger]b_{\text{in}}(t) - \sqrt{v\kappa_1}b_{\text{in}}^\dagger(t)[s_{mn}, a] \\ &\quad + \sqrt{v\kappa_2}[s_{mn}, a^\dagger]c_{\text{in}}(t) - \sqrt{v\kappa_2}c_{\text{in}}^\dagger(t)[s_{mn}, a]. \end{aligned}$$

Master equation

$$\begin{aligned}\frac{d}{dt}s_{mn} = & \frac{-i}{\hbar}[s_{mn}, \mathcal{H}_{\text{sys}}(t)] + \frac{\kappa}{2}(2a^\dagger s_{mn}a - s_{mn}a^\dagger a - a^\dagger a s_{mn}) \\ & + \sqrt{v\kappa_1}[s_{mn}, a^\dagger]b_{\text{in}}(t) - \sqrt{v\kappa_1}b_{\text{in}}^\dagger(t)[s_{mn}, a] \\ & + \sqrt{v\kappa_2}[s_{mn}, a^\dagger]c_{\text{in}}(t) - \sqrt{v\kappa_2}c_{\text{in}}^\dagger(t)[s_{mn}, a].\end{aligned}$$



rotating frame

$$s_{mn}(t) \equiv e^{i\Omega_0(m-n)t}S_{mn}(t), \quad a(t) \equiv e^{-i\Omega_0 t}A(t),$$

$$b_{\text{in}}(t) \equiv e^{-i\Omega_0 t}B_{\text{in}}(t), \quad c_{\text{in}}(t) \equiv e^{-i\Omega_0 t}C_{\text{in}}(t)$$



take expectation value

$$\sqrt{v}\langle B_{\text{in}} \rangle = E_{\text{in}} \text{ and } \langle C_{\text{in}} \rangle = 0,$$

$$\begin{aligned}\frac{d}{dt}\langle S_{mn} \rangle = & \frac{i}{\hbar}\langle [\mathcal{H}_{\text{sys}}, S_{mn}] \rangle + \frac{\kappa}{2}\left(2\langle A^\dagger S_{mn}A \rangle - \langle S_{mn}A^\dagger A \rangle - \langle A^\dagger A S_{mn} \rangle\right) \\ & + \sqrt{\kappa_1}E_{\text{in}}\langle [S_{mn}, A^\dagger] \rangle - \sqrt{\kappa_1}E_{\text{in}}^*\langle [S_{mn}, A] \rangle.\end{aligned}$$

Master equation

$$\begin{aligned}\frac{d}{dt} \langle S_{mn} \rangle &= \frac{i}{\hbar} \langle [\mathcal{H}_{\text{sys}}, S_{mn}] \rangle + \frac{\kappa}{2} \left(2 \langle A^\dagger S_{mn} A \rangle - \langle S_{mn} A^\dagger A \rangle - \langle A^\dagger A S_{mn} \rangle \right) \\ &\quad + \sqrt{\kappa_1} E_{\text{in}} \langle [S_{mn}, A^\dagger] \rangle - \sqrt{\kappa_1} E_{\text{in}}^* \langle [S_{mn}, A] \rangle.\end{aligned}$$



$$\langle S_{mn} \rangle = \text{Tr}[\rho S_{mn}] = \rho_{nm},$$

$$\langle A^\dagger S_{mn} A \rangle = \sqrt{(m+1)(n+1)} \text{Tr}[\rho S_{m+1,n+1}] = \sqrt{(m+1)(n+1)} \rho_{n+1,m+1},$$

etc.

$$\frac{d\rho}{dt} = -\frac{i}{\hbar} [\mathcal{H}_{\text{int}}, \rho] + \frac{\kappa}{2} (2A\rho A^\dagger - A^\dagger A \rho - \rho A^\dagger A),$$

Lindblad operator for single photon decay $D[\hat{a}]\rho$

$$\mathcal{H}_{\text{int}}/\hbar = \frac{\beta}{2} (A^2 + A^{\dagger 2}) + \frac{K}{2} A^\dagger A^\dagger A A + \sqrt{\kappa_1} (E_{\text{in}} A^\dagger + E_{\text{in}}^* A)$$

parametric drive Kerr nonlinearity single-photon drive

Analytical solution for steady state

PHYSICAL REVIEW A 94, 033841 (2016)



Exact steady state of a Kerr resonator with one- and two-photon driving and dissipation: Controllable Wigner-function multimodality and dissipative phase transitions

Nicola Bartolo,^{*} Fabrizio Minganti, Wim Casteels, and Cristiano Ciuti[†]

Université Paris Diderot, Sorbonne Paris Cité, Laboratoire Matériaux et Phénomènes Quantiques, CNRS-UMR7162, 75013 Paris, France

(Received 28 July 2016; published 22 September 2016)

N. Bartolo et al., Phys. Rev. A94, 033841 (2016).
<https://journals.aps.org/pra/abstract/10.1103/PhysRevA.94.033841>

Fig. 1

$$\hat{\mathcal{H}} = -\Delta \hat{a}^\dagger \hat{a} + \frac{U}{2} \hat{a}^\dagger \hat{a}^\dagger \hat{a} \hat{a} + F \hat{a}^\dagger + F^* \hat{a} + \frac{G}{2} \hat{a}^\dagger \hat{a}^\dagger + \frac{G^*}{2} \hat{a} \hat{a},$$
$$i \frac{\partial \hat{\rho}}{\partial t} = [\hat{\mathcal{H}}, \hat{\rho}] + i \frac{\gamma}{2} \mathcal{D}(\hat{a}) \hat{\rho} + i \frac{\eta}{2} \mathcal{D}(\hat{a}^2) \hat{\rho}, \quad = 0$$

for steady state



$$\langle \hat{a}^\dagger i \hat{a}^j \rangle = \frac{1}{N} \sum_{m=0}^{\infty} \frac{2^m}{m!} \mathcal{F}_{m+j}(f, g, c) \mathcal{F}_{m+i}^*(f, g, c).$$

$$\mathcal{F}_m(f, g, c) = (i\sqrt{g})^m {}_2F_1(-m, -c - i f/\sqrt{g}; -2c; 2),$$

${}_2F_1$: Gauss hypergeometric function

N. Bartolo et al., Phys. Rev. A94, 033841 (2016).
<https://journals.aps.org/pra/abstract/10.1103/PhysRevA.94.033841>

Fig. 2

Realization of quantum parametric oscillator

PHYSICAL REVIEW X 9, 021049 (2019)

Quantum Dynamics of a Few-Photon Parametric Oscillator

Zhaoyou Wang,^{*} Marek Pechal,^{*} E. Alex Wollack, Patricio Arrangoiz-Arriola,
Maodong Gao, Nathan R. Lee, and Amir H. Safavi-Naeini[†]

*Department of Applied Physics and Ginzton Laboratory, Stanford University
348 Via Pueblo Mall, Stanford, California 94305, USA*

Z. Wang et al., Phys. Rev. X 9, 021049 (2019).
<https://journals.aps.org/prx/abstract/10.1103/PhysRevX.9.021049>
Fig. 4c

- ◆ $K/\kappa \sim 17$: single-photon Kerr regime
- ◆ no ancilla qubit
 - state tomography based on transient PSD measurement
- ◆ 5.8 photon Schrodinger's cat state

Z. Wang et al., Phys. Rev. X 9, 021049 (2019).
<https://journals.aps.org/prx/abstract/10.1103/PhysRevX.9.021049>

Fig. 5

Z. Wang et al., Phys. Rev. X 9, 021049 (2019).
<https://journals.aps.org/prx/abstract/10.1103/PhysRevX.9.021049>

Figs. 3a and 3b

Z. Wang et al., Phys. Rev. X 9, 021049 (2019).

<https://journals.aps.org/prx/abstract/10.1103/PhysRevX.9.021049>

Fig. 4d

Table of Contents

1. Brief overview
2. Introduction of KPO
 - theoretical description
3. Application of KPO in FTQC
4. Application of KPO in quantum annealing
5. Summary

Hardware-efficient quantum error correction

Generic QEC

Hardware efficient QEC

W. Cai et al., Fundamental Research **1**, 50 (2021).
<https://www.sciencedirect.com/science/article/pii/S2667325820300145>
Figs. 2a and 2b

Encode logical qubit using multiple physical qubits (two-level system)
→increase in error source
→requires many physical qubits

Encode logical qubit using one physical system with infinite degree of freedom
→limited error source (**with biased noise**)
→reduced hardware overhead

W. Cai et al., Fundamental Research **1**, 50 (2021).

noise-biased qubit

Coherent state $|\alpha\rangle = e^{-\frac{1}{2}|\alpha|^2} \sum_{n=0}^{\infty} \frac{\alpha^n}{\sqrt{n!}} |n\rangle$

N. Frattini, PhD thesis 2021
https://elischolar.library.yale.edu/gsas_dissertations/332/
Fig. 4.1a

$$|\pm X\rangle = \frac{1}{\sqrt{2}} \left(|c_\alpha^+\rangle \pm |c_\alpha^-\rangle \right) \rightarrow |\pm\alpha\rangle$$

$$|\pm Y\rangle = \frac{1}{\sqrt{2}} \left(|c_\alpha^+\rangle \pm i |c_\alpha^-\rangle \right) \rightarrow \frac{1}{\sqrt{2}} (|+\alpha\rangle \mp i |-\alpha\rangle)$$

$$|\pm Z\rangle = |c_\alpha^\pm\rangle \rightarrow \frac{1}{\sqrt{2}} (|+\alpha\rangle \pm |-\alpha\rangle)$$

Eigenstate of photon loss operator

$$a|\alpha\rangle = \alpha|\alpha\rangle$$

quasi-orthogonal

$$\langle -\alpha | \alpha \rangle = e^{-2|\alpha|^2} \sim 0$$

error due to photon loss

Phase-flip rate:

$$|\langle -\alpha | a | \alpha \rangle|^2 = |\alpha|^2 e^{-4|\alpha|^2} \sim 0$$
 exponentially suppressed

Bit-flip rate:

$$|\langle c_\alpha^- | a | c_\alpha^+ \rangle|^2 \sim |\alpha|^2$$
 polynomial increase

Can focus on most likely error  higher error threshold

noise-biased qubit

N. Frattini, PhD thesis 2021

◆ Operators in cat basis: ex. $\begin{pmatrix} \langle \mathcal{C}_\alpha^+ | a | \mathcal{C}_\alpha^+ \rangle & \langle \mathcal{C}_\alpha^+ | a | \mathcal{C}_\alpha^- \rangle \\ \langle \mathcal{C}_\alpha^- | a | \mathcal{C}_\alpha^- \rangle & \langle \mathcal{C}_\alpha^- | a | \mathcal{C}_\alpha^+ \rangle \end{pmatrix} = \alpha \begin{pmatrix} 0 & r^{-1} \\ r & 0 \end{pmatrix} = \alpha \left(\frac{r + r^{-1}}{2} \right) \mathbf{X} - i\alpha \left(\frac{r - r^{-1}}{2} \right) \mathbf{Y}$

N. Frattini, PhD thesis 2021

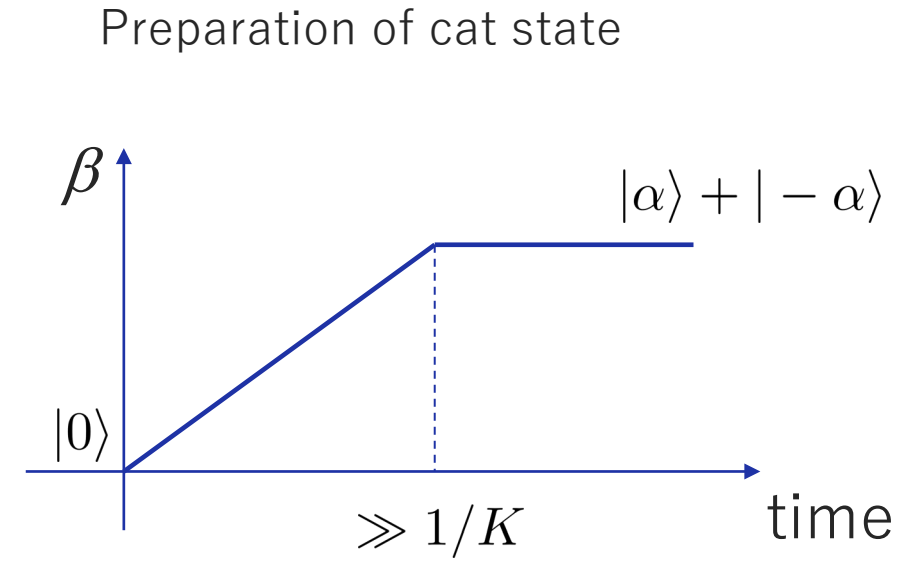
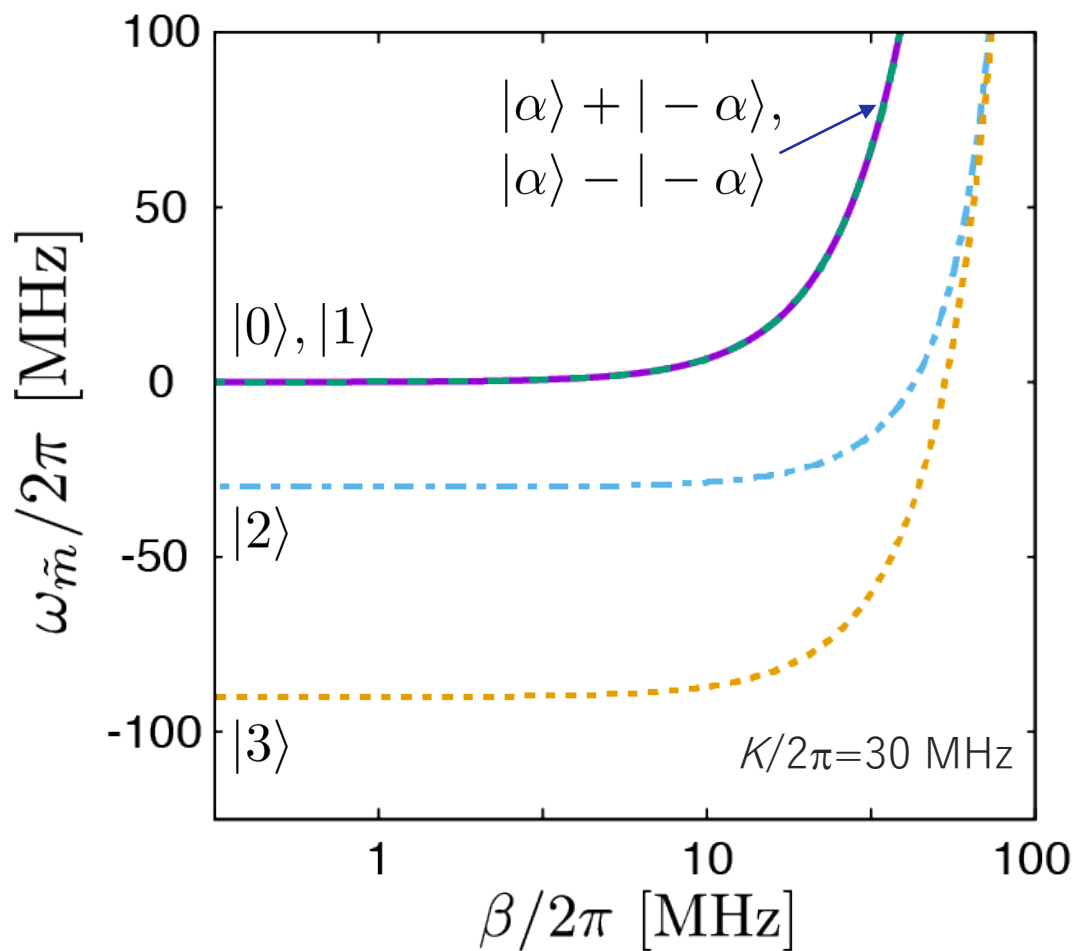
https://elischolar.library.yale.edu/gsas_dissertations/332/

Table 4.1

$$\begin{aligned} |\mathcal{C}_\alpha^\pm\rangle &= \mathcal{N}_\alpha^\pm (|\alpha\rangle \pm |-\alpha\rangle) & r &\rightarrow \begin{cases} 1 - e^{-2|\alpha|^2} & (\text{large } \alpha) \\ 0 & (\alpha \rightarrow 0) \end{cases} & r^2 &\rightarrow \begin{cases} 1 - 2e^{-2|\alpha|^2} & (\text{large } \alpha) \\ 0 & (\alpha \rightarrow 0) \end{cases} \\ \mathcal{N}_\alpha^\pm &= 1/\sqrt{2(1 \pm e^{-2|\alpha|^2})} & r^{-1} &\rightarrow \begin{cases} 1 + e^{-2|\alpha|^2} & (\text{large } \alpha) \\ 1/|\alpha| & (\alpha \rightarrow 0) \end{cases} & r^{-2} &\rightarrow \begin{cases} 1 + 2e^{-2|\alpha|^2} & (\text{large } \alpha) \\ 1/|\alpha|^2 & (\alpha \rightarrow 0) \end{cases} \\ r &= \mathcal{N}_\alpha^+ / \mathcal{N}_\alpha^- \end{aligned}$$

Gate operations

$$\mathcal{H}_{\text{KPO}}/\hbar = -\frac{K}{2}a^\dagger a^\dagger a a + \beta(a^{\dagger 2} + a^2)$$



R_x gate

P. T. Cochrane et al., Phys. Rev. A **59**, 2631 (1999).
 H. Goto, Sci. Rep. **6**, 21686 (2016).
 S. Puri et al., npj Quantum Info. **3**, 18 (2017).

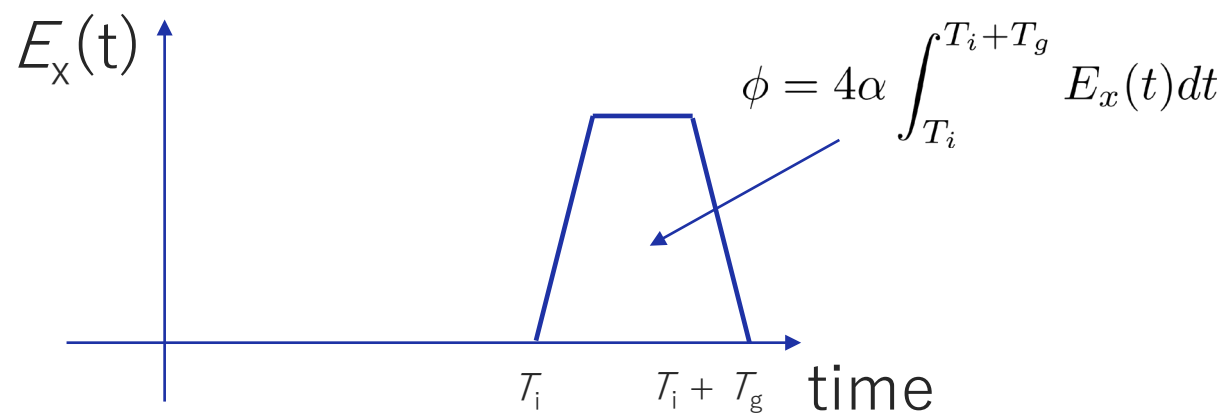
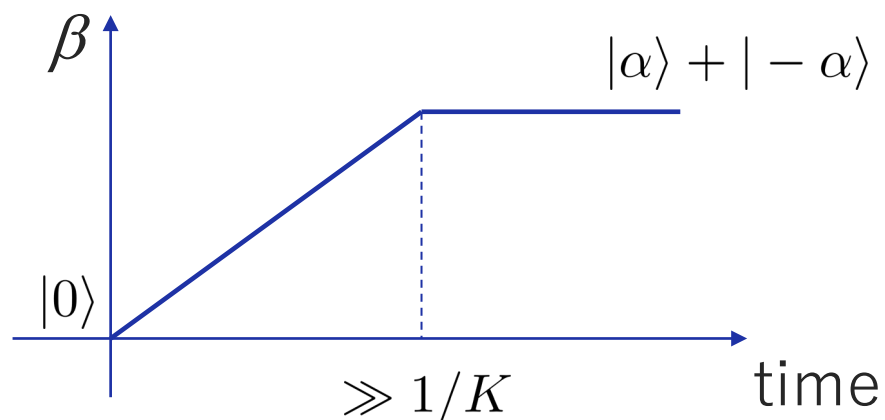
single-photon drive @ $\omega_p/2$

$$\mathcal{H}_{\text{KPO}}/\hbar = -\frac{K}{2}a^\dagger a^\dagger aa + \beta(a^{\dagger 2} + a^2) + E_x(t)(a + a^\dagger)$$

produces energy difference between $|\alpha\rangle$ and $|-\alpha\rangle$

$$\langle \alpha | E_x(t)(a + a^\dagger) | \alpha \rangle = 2\alpha E_x(t)$$

$$\langle -\alpha | E_x(t)(a + a^\dagger) | -\alpha \rangle = -2\alpha E_x(t)$$

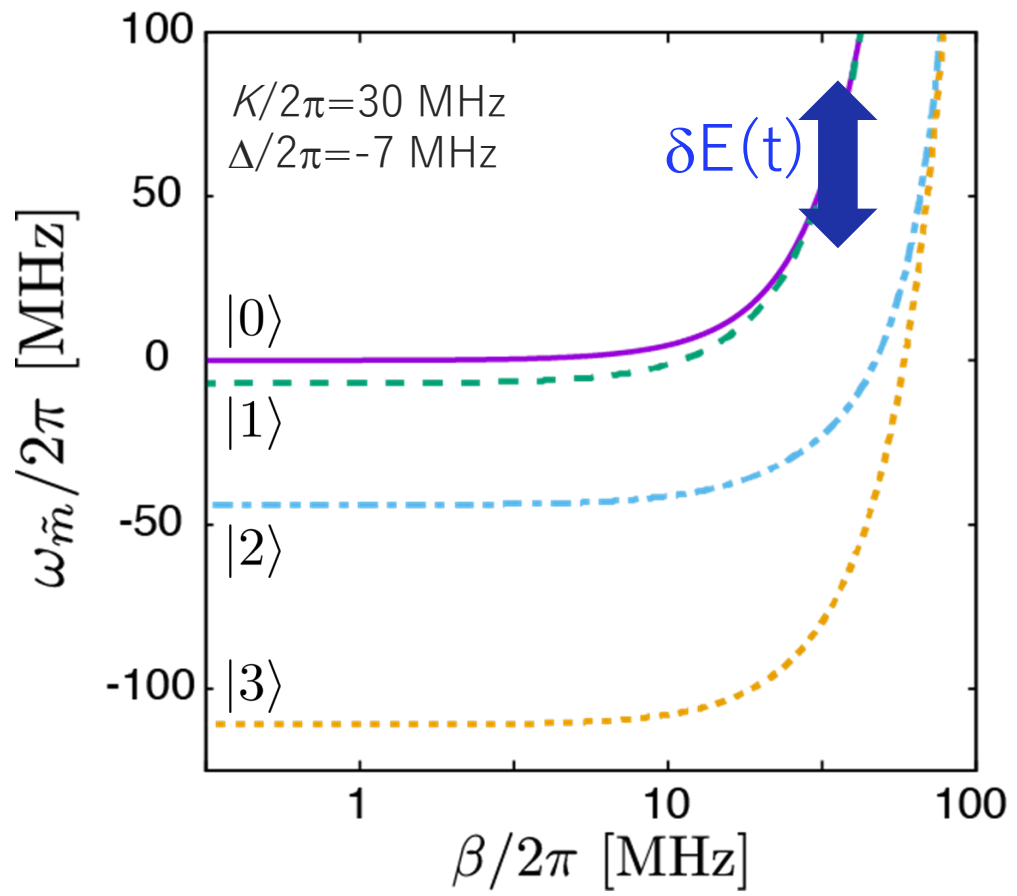


$$H \begin{pmatrix} e^{-i\phi/2} & 0 \\ 0 & e^{i\phi/2} \end{pmatrix} H = \begin{pmatrix} \cos \frac{\phi}{2} & -i \sin \frac{\phi}{2} \\ -i \sin \frac{\phi}{2} & \cos \frac{\phi}{2} \end{pmatrix} = R_x(\phi)$$

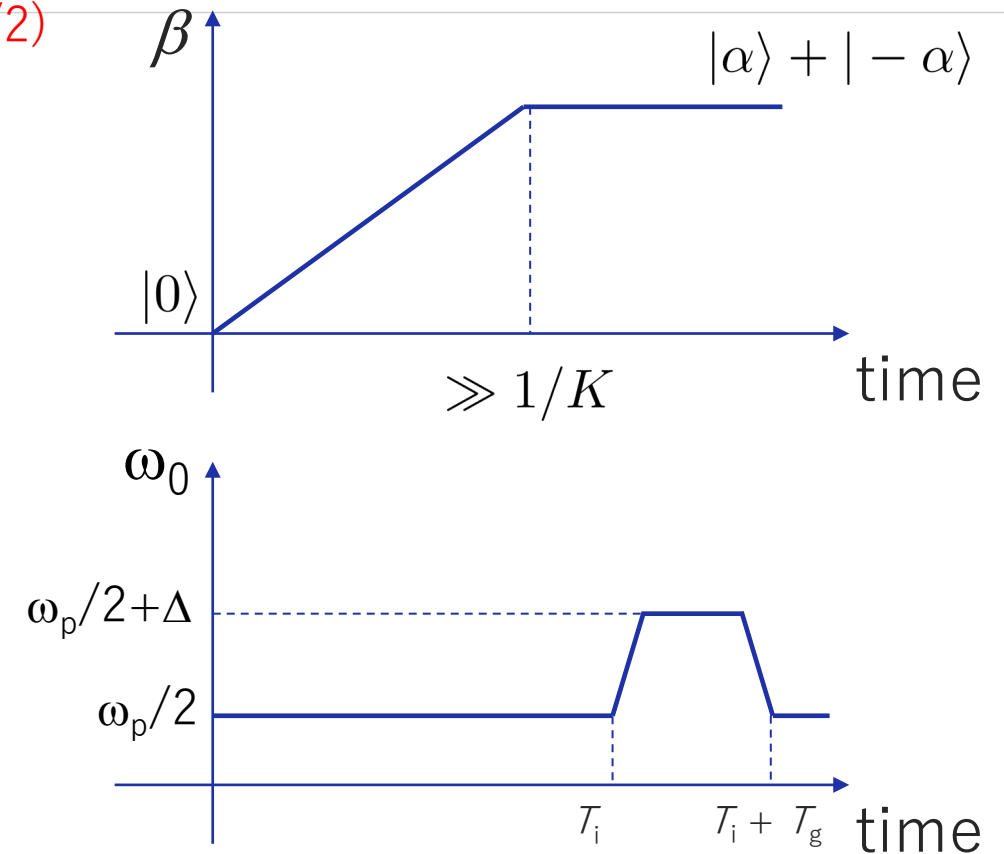
in α basis change to cat basis

R_z gate

$$\mathcal{H}_{\text{KPO}}/\hbar = -\frac{K}{2}a^\dagger a^\dagger aa + \beta(a^{\dagger 2} + a^2) + \Delta(t)a^\dagger a$$



H. Goto, Sci. Rep. **6**, 21686 (2016).
S. Puri et al., npj Quantum Info. **3**, 18 (2017).



$$\begin{pmatrix} e^{-i\theta/2} & 0 \\ 0 & e^{i\theta/2} \end{pmatrix} \quad \theta = \int_{T_i}^{T_i+T_g} \delta E(t) dt$$

Alternative method:
temporarily remove the two-photon drive. Grim et al., 2020

Two-qubit R_{zz} gate

1. H. Goto, Sci. Rep. **6**, 21686 (2016).
2. S. Puri et al., npj Quantum Info. **3**, 18 (2017).
3. H. Chono et al., Phys. Rev. Res. **4**, 043054 (2022).
4. S. Puri et al., Sci. Adv. **6**, eaay5901 (2020). [bias preserving C-NOT gate]

- ◆ R_{zz} gate (in α basis) based on linear coupling ($a_1 a_2^+ + a_1^+ a_2$) was proposed in Refs. [1,2].
 - requires temporal control of the coupling $g(t)$ to turn on/off the coupling
- ◆ Effective turn on/off using conditional-driving [3]
 - large detuning between two KPO's effectively turns off the coupling in idle state
 - additional two-photon drive at sum (or diff.) frequency induces the coupling
 - realize R_{zz} gate (in α basis)

$$\begin{pmatrix} |\alpha\rangle|\alpha\rangle & |\alpha\rangle|-\alpha\rangle & |- \alpha\rangle|\alpha\rangle & |- \alpha\rangle|-\alpha\rangle \\ e^{-i\theta/2} & 0 & 0 & 0 \\ 0 & e^{i\theta/2} & 0 & 0 \\ 0 & 0 & e^{i\theta/2} & 0 \\ 0 & 0 & 0 & e^{-i\theta/2} \end{pmatrix}$$

$$\hat{H} = \sum_{j=1,2} \hat{H}_j + \hat{H}_I + \hat{H}_g,$$

$$\frac{\hat{H}_j}{\hbar} = -\frac{K}{2}\hat{a}_j^{\dagger 2}\hat{a}_j^2 + \frac{P}{2}(\hat{a}_j^{\dagger 2} + \hat{a}_j^2),$$

$$\frac{\hat{H}_I}{\hbar} = g(\hat{a}_1\hat{a}_2^\dagger e^{-i\Delta_{12}t} + \hat{a}_1^\dagger\hat{a}_2 e^{i\Delta_{12}t}),$$

$$\frac{\hat{H}_g}{\hbar} = \frac{p_g(t)}{2}(\hat{a}_1^2 e^{-i\Delta_{12}t} + \hat{a}_1^{\dagger 2} e^{i\Delta_{12}t}),$$

static coupling:
effectively off due to **fast oscillation**

**cancel the oscillation
to turn on the coupling**



$$\alpha_1 \rightarrow \alpha_1 + \delta\alpha_1 e^{i\Delta_{12}t}$$

additional two-photon drive:

H. Chono et al., Phys. Rev. Res. 4, 043054 (2022).
<https://journals.aps.org/prresearch/abstract/10.1103/PhysRevResearch.4.043054>
 Fig. 1

Stabilization and operation of a Kerr-cat qubit

A. Grimm *et al.*, Nature **584**, 205 (2020).

- ◆ Use SNAIL's 2nd order and 3rd order nonlinearities to realize two-photon drive and Kerr nonlinearity.
- ◆ Readout after transforming to Fock-base qubit (adiabatically turn off the pump) or freq. conversion using 3-wave mixing.
- ◆ phase-flip time \gg bit-flip time (qubit with biased noise)
- ◆ two-photon drive increases phase-flip time by >30 times compared to T2 of FQ (stabilization)

A. Grimm *et al.*, Nature **584**, 205 (2020).
<https://www.nature.com/articles/s41586-020-2587-z>
Figs. 1d, 1e, and 1f

R_x gate

A. Grimm *et al.*, Nature **584**, 205 (2020).
<https://www.nature.com/articles/s41586-020-2587-z>
Figs. 2a, 2b, and 2c

A. Grimm *et al.*, Nature **584**, 205 (2020).
<https://www.nature.com/articles/s41586-020-2587-z>
Figs. 4b, 4c, 4f, and 4g

phase-flip time
~100 us

bit-flip time
~2.6 us

Table of Contents

1. Brief overview
2. Introduction of KPO
 - theoretical description
3. Application of KPO in FTQC
4. Application of KPO in quantum annealing
5. Summary

Quantum bifurcation machine

Bifurcation-based adiabatic quantum computation with a nonlinear oscillator network

Hayato Goto

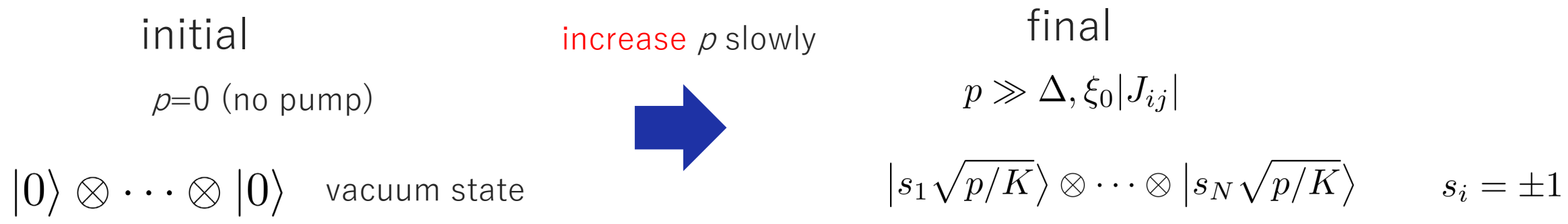
Sci. Rep. **6**, 21686 (2016).

Network of KPO's: connected by linear coupling

$$H_1 = \hbar\Delta a^\dagger a + \frac{\hbar K}{2}a^{\dagger 2}a^2 - \frac{\hbar P}{2}(a^2 + a^{\dagger 2})$$

$$H = \sum_{i=1}^N H_1^{(i)} - \frac{\hbar\xi_0}{2} \sum_{i=1}^N \sum_{j=1}^N J_{i,j} (a_i^\dagger a_j + a_i a_j^\dagger)$$

$$\Delta_i = \xi_0 \sum_{j=1}^N |J_{i,j}| \quad \text{for the vacuum state to be the ground state}$$



$$E_{\text{corr}}(\{s_i\}) = \hbar \frac{P}{K} \sum_{i=1}^N \Delta_i - \hbar \xi_0 \frac{P}{K} \sum_{i=1}^N \sum_{j=1}^N J_{i,j} s_i s_j$$

should be minimized!

Quantum bifurcation machine

Bifurcation-based adiabatic quantum computation with a nonlinear oscillator network

Hayato Goto

Sci. Rep. **6**, 21686 (2016).

numerical simulation for 4-spin problem

1000 instances with random J_{ij}

KPO
(quantum)
finds global minimum

Quantum effect?

classical
trapped in local minimum

H. Goto, Sci. Rep. **6**, 21686 (2016).
<https://www.nature.com/articles/srep21686>

Figs. 3a and 3b

H. Goto, Sci. Rep. **6**, 21686 (2016).
<https://www.nature.com/articles/srep21686>
Fig. 2

Ising machine using OPO

For theoretical comparison between QbM and CIM,
see Goto, J. Phys. Soc. Jpn. **88**, 061015 (2019).

OPTICAL PROCESSING

A coherent Ising machine for 2000-node optimization problems

Takahiro Inagaki,^{1*} Yoshitaka Haribara,^{2,3,4} Koji Igarashi,⁵ Tomohiro Sonobe,^{4,6}
Shuhei Tamate,⁴ Toshimori Honjo,¹ Alireza Marandi,⁷ Peter L. McMahon,⁷
Takeshi Umeki,⁸ Koji Enbutsu,⁸ Osamu Tadanaga,⁸ Hirokazu Takenouchi,⁸
Kazuyuki Aihara,^{2,3} Ken-ichi Kawarabayashi,^{4,6} Kyo Inoue,⁵
Shoko Utsunomiya,⁴ Hiroki Takesue^{1*}

P. L. McMahon *et al.*, Science **354**, 614 (2016).
<https://www.science.org/doi/full/10.1126/science.aah5178>
Fig. 1

T. Inagaki et al.,
<https://www.science.org/doi/10.1126/science.aah4243>
Fig. 2A

T. Inagaki et al.,
<https://www.science.org/doi/10.1126/science.aah4243>
Fig. 4

Simulated bifurcation machine

H. Goto *et al*, Sci. Adv. **5**, eaav2372 (2019),
also H. Goto *et al*, Sci. Adv. **7**, eabe79532 (2021).

SCIENCE ADVANCES | RESEARCH ARTICLE

APPLIED PHYSICS

Combinatorial optimization by simulating adiabatic bifurcations in nonlinear Hamiltonian systems

Hayato Goto*, Kosuke Tatsumura, Alexander R. Dixon

H. Goto *et al*, Sci. Adv. **5**, eaav2372 (2019).
<https://www.science.org/doi/10.1126/sciadv.aav2372>
Eqs. 3, 4, and 5

H. Goto *et al*, Sci. Adv. **5**, eaav2372 (2019).
<https://www.science.org/doi/10.1126/sciadv.aav2372>
Fig. 2

All-to-all connectivity

- ◆ Minor embedding
 - V. Choi, Quantum Inf Process **10**, 343 (2011).
- ◆ Measurement and feedback
 - T. Inagaki *et al.*, Science **354**, 603 (2016).
- ◆ Bus coupling
 - T. Onodera *et al.*, NPJ Quantum Inf. **6**, 48 (2020).
- ◆ Parity mapping
 - W. Lechner *et al.*, Sci. Adv. **1** e1500838 (2015).

Lechner-Hauke-Zoller (LHZ) scheme

RESEARCH ARTICLE

Sci. Adv. **1**, e1500838 (2015).

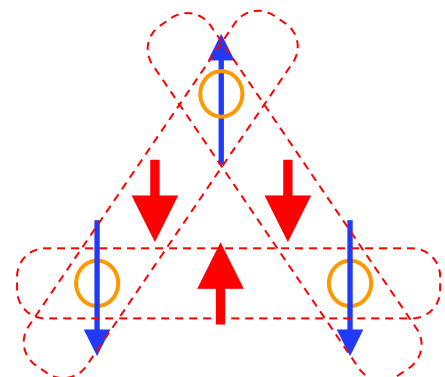
QUANTUM MECHANICS

A quantum annealing architecture with all-to-all connectivity from local interactions

Wolfgang Lechner,^{1,2*} Philipp Hauke,^{1,2} Peter Zoller^{1,2}

- ◆ Define new pseudo-spins for all pairs of spins in the network by their parity (parallel or anti-parallel)

example:
3 spins

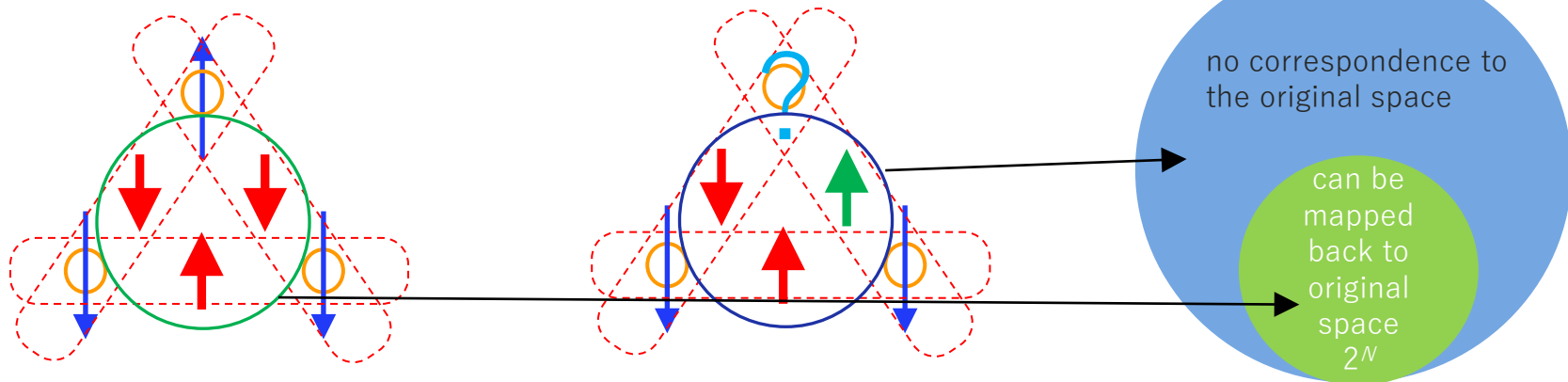


$$\sum_{i < j}^N J_{ij} \sigma_{iz} \sigma_{jz} \quad \xrightarrow{\hspace{1cm}} \quad \sum_k^{N C_2} J_k \tilde{\sigma}_{kz}$$

coupled 2 spins single spin + local field
of spins: N **# of spins: $N C_2 \sim O(N^2)$**

Lechner-Hauke-Zoller (LHZ) scheme

- ◆ Mapping makes the Hilbert space larger.



- ◆ We need constraint!

$$\sum_{i < j}^N J_{ij} \sigma_{iz} \sigma_{jz}$$

Mapping
→

$$\mathcal{H}_p = \sum_k^K J_k \tilde{\sigma}_{kz} + \sum_l^{K-N+1} C_l$$

Original problem

penalty term to make the energy
of the blue region higher

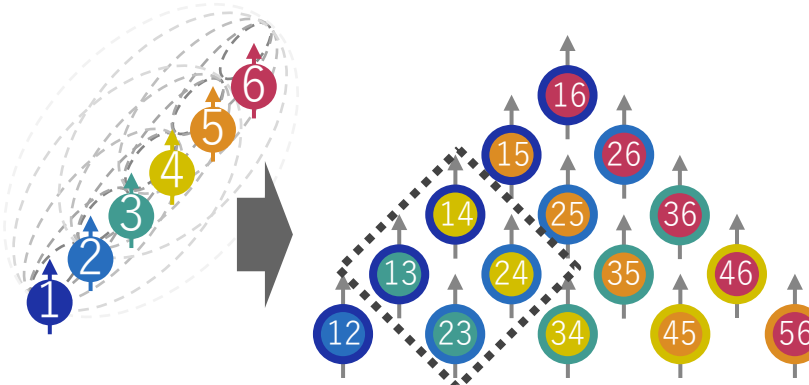
Lechner-Hauke-Zoller (LHZ) scheme

W. Lechner *et al.*, Sci. Adv. **1** e1500838 (2015).

- ◆ Express the product (parity) of two Ising spins σ using one physical spin $\tilde{\sigma}$
- ◆ Realize programmable all-to-all connectivity with local interactions.
- ◆ Simple correspondence between physical and logical spins

$$\mathcal{H} = - \sum_{i < j} J_{ij} \sigma_i \sigma_j = - \sum_k J_k \tilde{\sigma}_k$$

interaction J_{ij} \rightarrow local field J_k
fully-connected
logical spin N \rightarrow $\frac{N(N-1)}{2}$ physical spins



- ◆ $\tilde{\sigma}$ must satisfy the following conditions

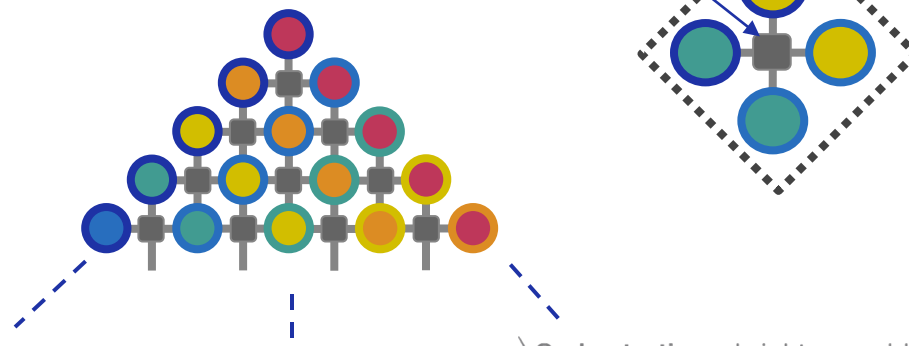
$$\tilde{\sigma}_{1,3} \tilde{\sigma}_{2,3} \tilde{\sigma}_{2,4} \tilde{\sigma}_{4,1} = \sigma_1^2 \sigma_2^2 \sigma_3^2 \sigma_4^2 = 1$$

$$\mathcal{H} = - \sum_k J_k \tilde{\sigma}_k - C \sum \tilde{\sigma}_a \tilde{\sigma}_b \tilde{\sigma}_c \tilde{\sigma}_d$$

four-body interaction
how to realize?

$$\tilde{\sigma}_{1,3} \tilde{\sigma}_{2,3} \tilde{\sigma}_{2,4} \tilde{\sigma}_{4,1} = 1$$

constraint



Quantum bifurcation machine with LHZ scheme

ARTICLE

Received 1 Nov 2016 | Accepted 28 Apr 2017 | Published 8 Jun 2017

DOI: 10.1038/ncomms15785

OPEN

Nature Commun. 8, 15785 (2017).

Quantum annealing with all-to-all connected nonlinear oscillators

Shruti Puri¹, Christian Kraglund Andersen², Arne L. Grimsmo¹ & Alexandre Blais^{1,3}

Josephson junction as a 4-body coupler

S. Puri et al., Nature Commun. 8, 15785 (2017).
<https://www.nature.com/articles/ncomms15785>

Fig. 4

S. Puri et al., Nature Commun. 8, 15785 (2017).
<https://www.nature.com/articles/ncomms15785>

Fig. 5

Quantum bifurcation machine with LHZ scheme

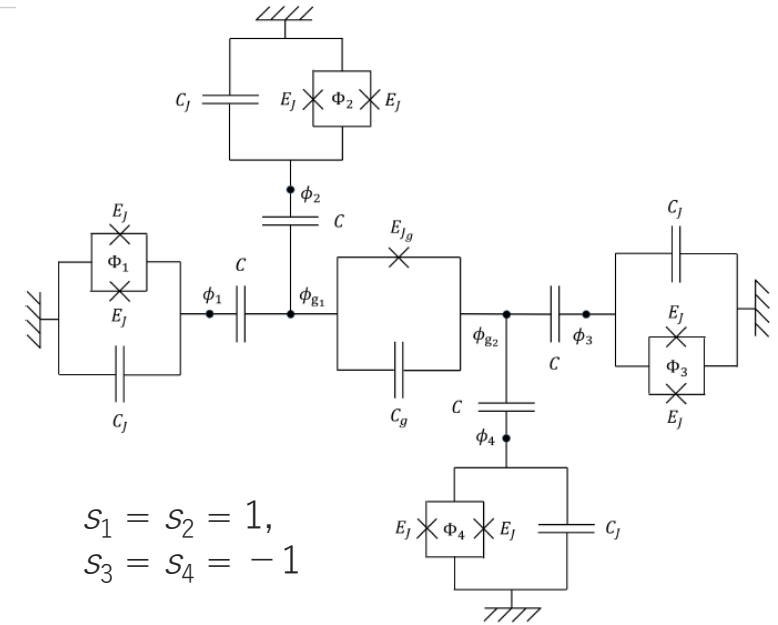
- ◆ 4-body coupler using a Josephson junction

$$H_{\text{total}} = \sum_{k=1..4} H_{\text{JPO},k} + H_{\text{coupler}} + g \sum_k s_k (a_k^+ - a_k)(a_g - a_g^+)$$

$$H_{\text{JPO},k} = \hbar\omega a_k^+ a_k - \frac{E_C}{12} (a_k^+ + a_k)^4 + \frac{\hbar\omega\delta E_J}{4E_J} (a_k^+ + a_k)^2 \cos(\omega_{p,k}t)$$

$$H_{\text{coupler}} = \hbar\omega_g a_g^+ a_g - \frac{E_{Cg}}{12} (a_g^+ + a_g)^4$$

coupler nonlinearity



$$\begin{aligned} s_1 &= s_2 = 1, \\ s_3 &= s_4 = -1 \end{aligned}$$

- ◆ Coupler's nonlinear term turns to the effective 4-body coupling by unitary transform $U_g = e^{g' \sum_k s_k (a_k^+ a_g - a_k a_g^+)}$ under small $g' = g/\hbar(\omega - \omega_g)$

$$\begin{aligned} (a_g^+ + a_g)^4 &\rightarrow \left(a_g^+ + g' \sum_k s_k a_k - 2g'^2 a_g + \dots + \text{h.c.} \right)^4 \\ &= (a_g^+ + a_g)^4 + 24g'^4 \left(a_1^+ a_2^+ a_3 a_4 + a_1 a_2 a_3^+ a_4^+ + \sum_{k < l} a_k^+ a_k a_l^+ a_l \right) + \dots \end{aligned}$$

Quantum bifurcation machine with LHZ scheme

◆ 4-body coupler using a Josephson junction

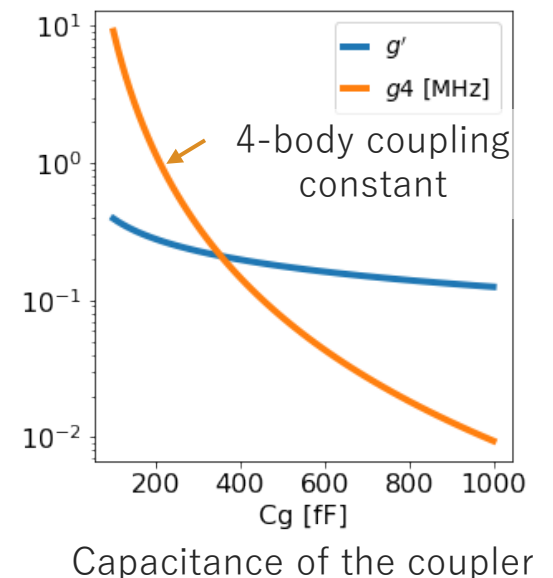
■ Effective Hamiltonian for JPOs in the frame rotating at $\omega_{p,k}/2$

$$H_{\text{total}} \rightarrow H'_{\text{total}} \simeq \sum_k H_{\text{JPO},k} + H'_{\text{coupler}}$$
$$-g^{(4)} \left(a_1^+ a_2^+ a_3 a_4 + a_1 a_2 a_3^+ a_4^+ + \sum_{k < l} a_k^+ a_k a_l^+ a_l \right)$$

- Condition for pump frequencies $\omega_{p,1} + \omega_{p,2} = \omega_{p,3} + \omega_{p,4}$ keeps the 4-body coupling terms stationary
- Other coupling terms oscillate fast and are ignored

■ 4-body coupling constant $g^{(4)} = 2g'^4 E_{C_g}$

- g' : Effective coupling constant between a JPO and the coupler
- E_{C_g} : Capacitive energy of the coupler
- Decreasing capacitance of the coupler can increase $g^{(4)}$ without increasing g' much



R. Miyazaki, AQC2022

Quantum bifurcation machine with LHZ scheme

◆ Advantages

- no on-chip coupler
 - J_{ij} and C are controlled by the phase of the injection microwave.
- neighboring KPO's have different resonance frequencies
 - smaller crosstalk
- state stabilized after pump becomes sufficiently high

◆ Issues

- Performance benchmarking with conventional quantum annealing
- decoherence during adiabatic evolution*?
- requires the same microwave engineering as gate-based QC without error correction

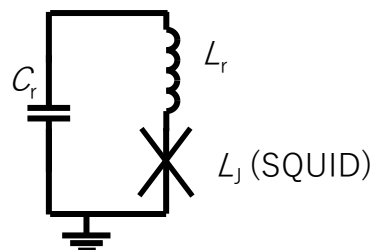
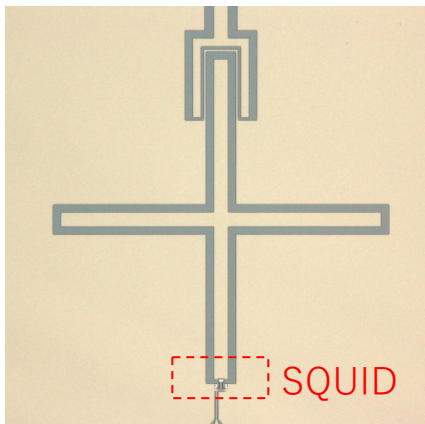
M. J. Kewming et al.,
New J. Phys. **22**, 053042 (2020).

*effect of photon loss is investigated in
S. Puri et al., Nature Commun. **8**, 15785 (2017).

JPO in single-photon Kerr regime (KPO)

- ◆ Kerr nonlinearity $K \gg$ photon-loss rate $\kappa \sim 2\pi \times 0.1$ MHz
- ◆ how to design Kerr nonlinearity?

lumped-element circuit



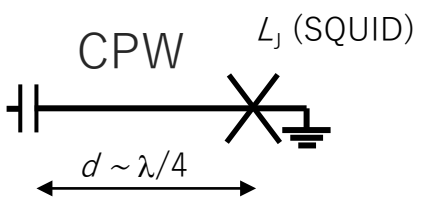
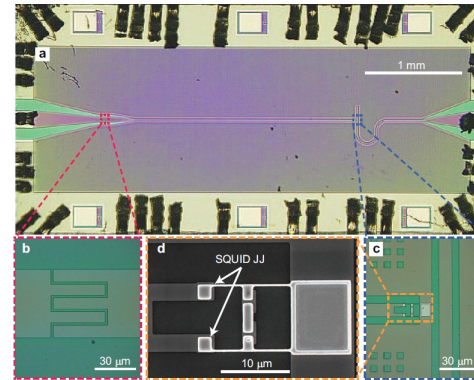
Kerr nonlinearity

$$\mathcal{H} = \hbar\omega'_0 \left(a^\dagger a + \frac{1}{2} \right) - \frac{E_c}{12} \left(\frac{L_J}{L_r + L_J} \right)^3 (a^\dagger + a)^4$$

$$\omega'_0 = \frac{1}{\sqrt{(L_r + L_J)C_r}}$$

C_J is neglected.

distributed-element circuit



SQUID

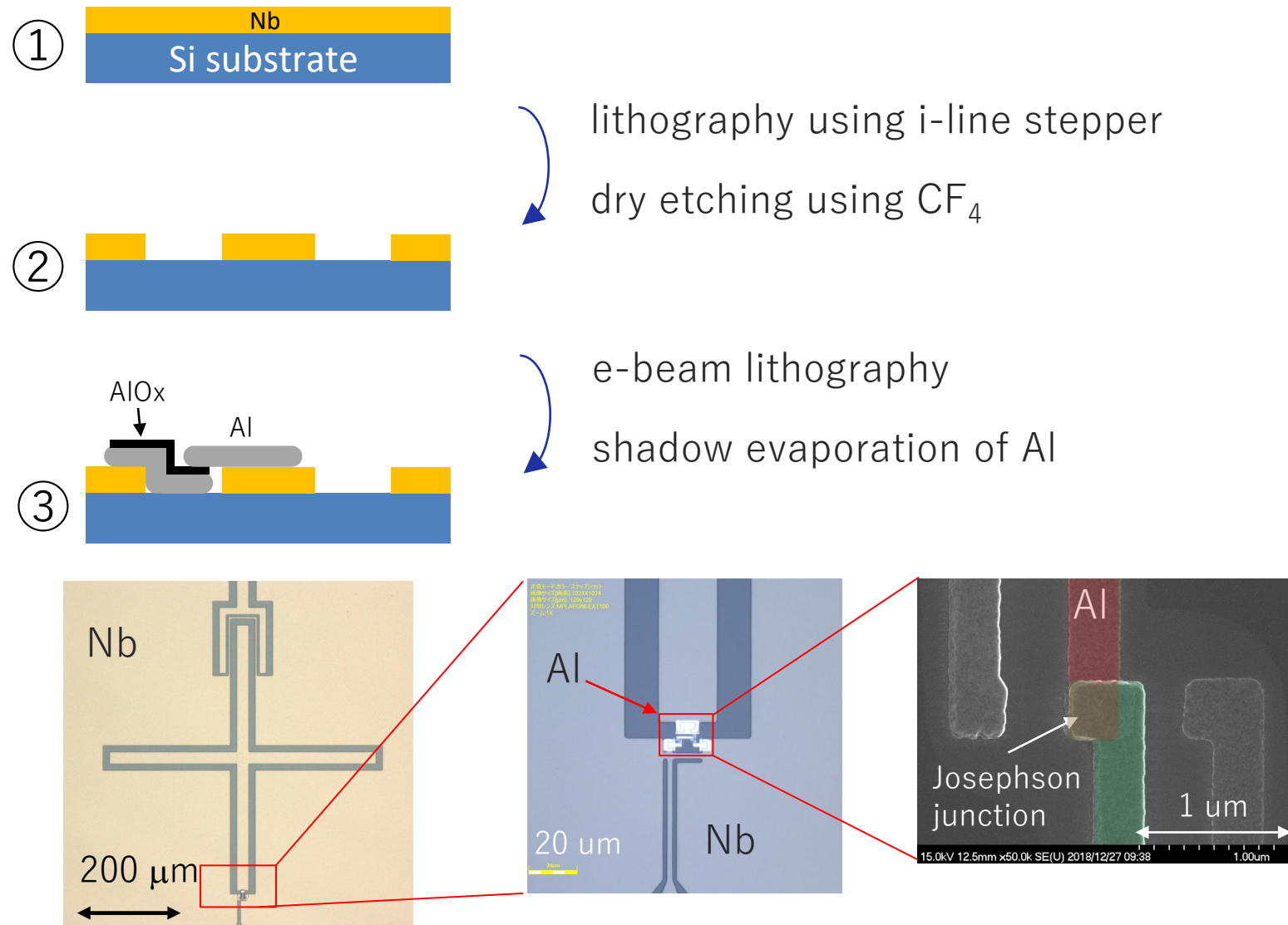
Kerr nonlinearity

$$\mathcal{H} = \hbar\omega_k \left(a^\dagger a + \frac{1}{2} \right) - E_c B_k (a^\dagger + a)^4$$

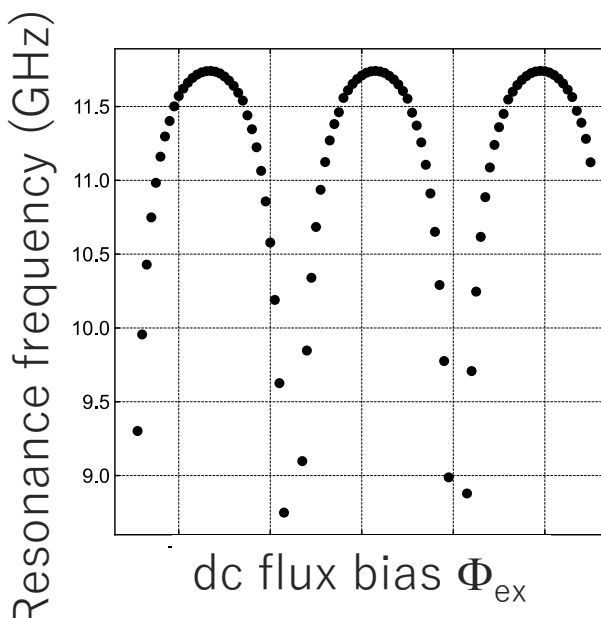
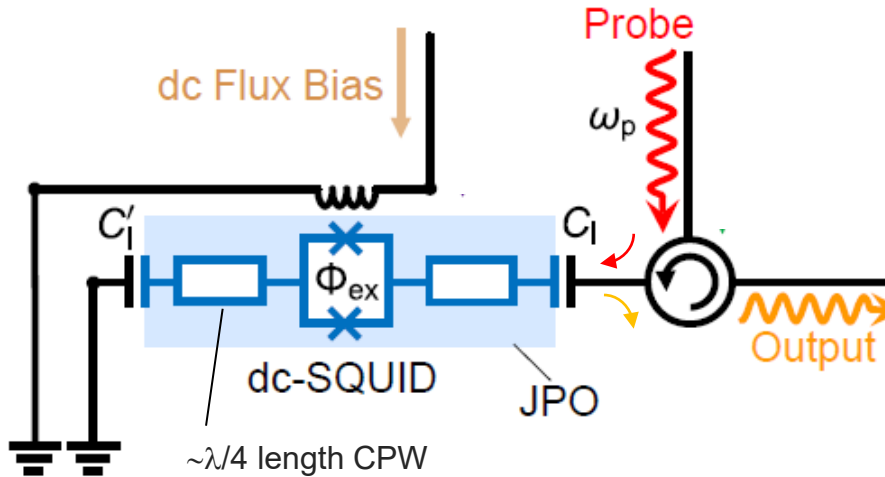
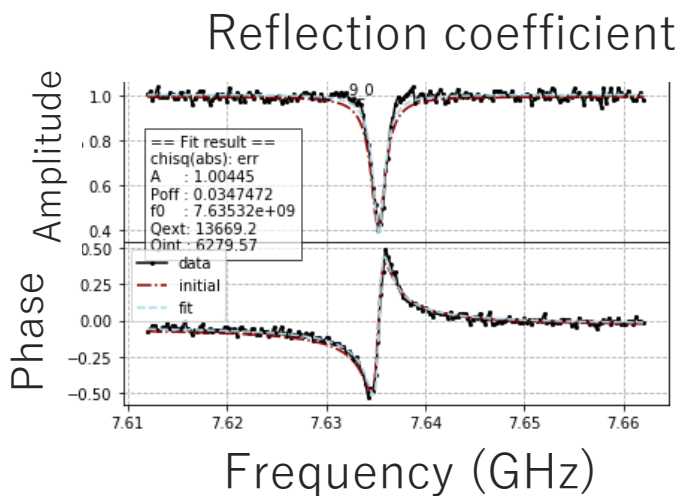
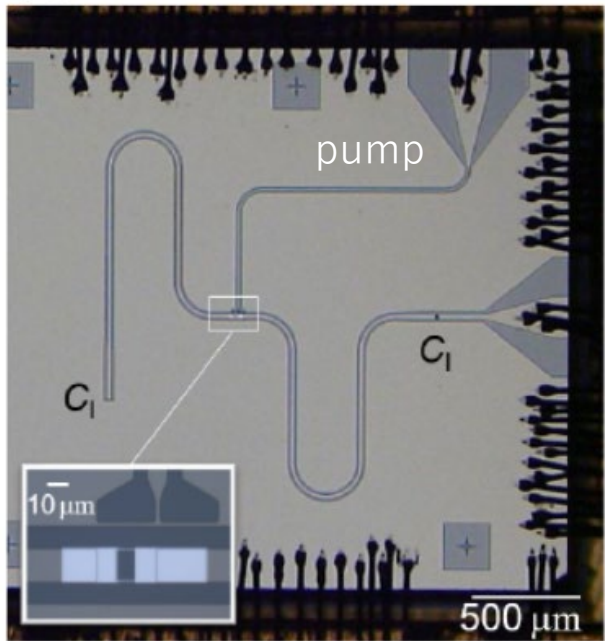
$$B_k = \frac{(1/4) \cos^2(kd)}{1 + 2kd/\sin(2kd)}$$

Wallquist et al., PRB **74**, 224506 (2006).
Bourassa et al., PRA **86**, 013814 (2012).

Device fabrication



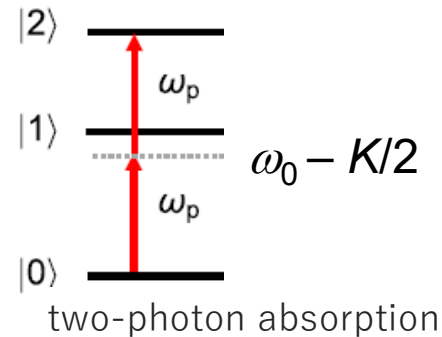
JPO in single-photon Kerr regime (KPO)



JPO in single-photon Kerr regime (KPO)

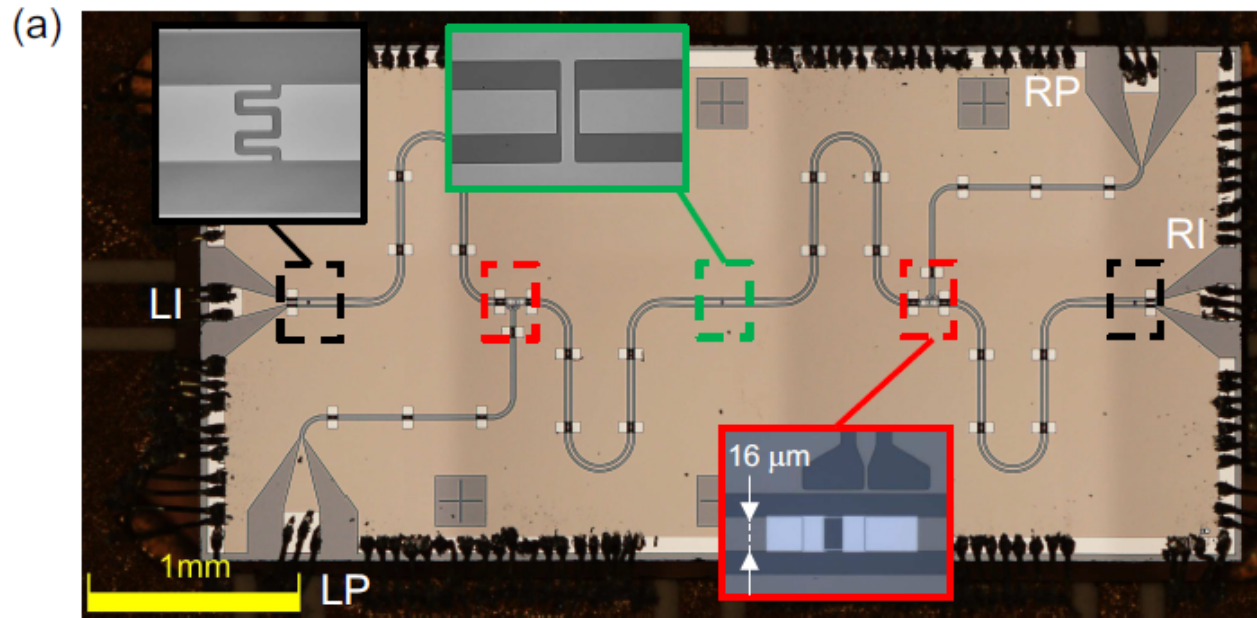
- ◆ Kerr coefficient (flux-bias dependent) can be extracted from the power dependence of reflection coefficient.
- ◆ Perfect agreement with theory
- ◆ Can be used as power calibration of probe microwave

T. Yamaji *et al.*, Phys. Rev. A **105**, 023519 (2022).
<https://journals.aps.org/prl/abstract/10.1103/PhysRevA.105.023519>
Figs. 3a, 3a', 3b, and 3b'

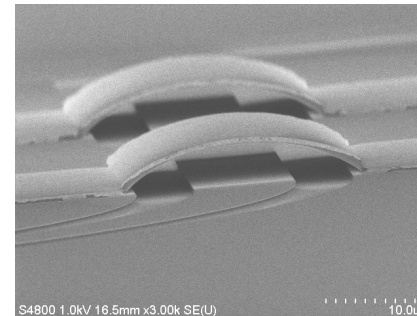


$$\mathcal{H} = \hbar\omega_0 a^\dagger a - \hbar \frac{K}{2} a^\dagger a^\dagger a a$$

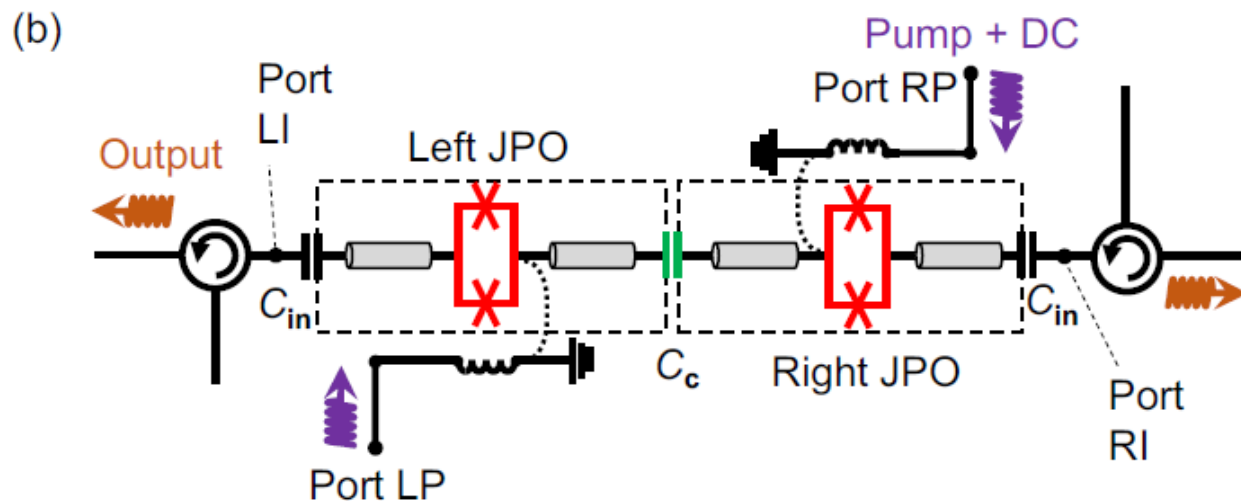
Coupled KPO's



Air-bridges



- suppress slot-line mode
- create superconducting loop to suppress x-talk

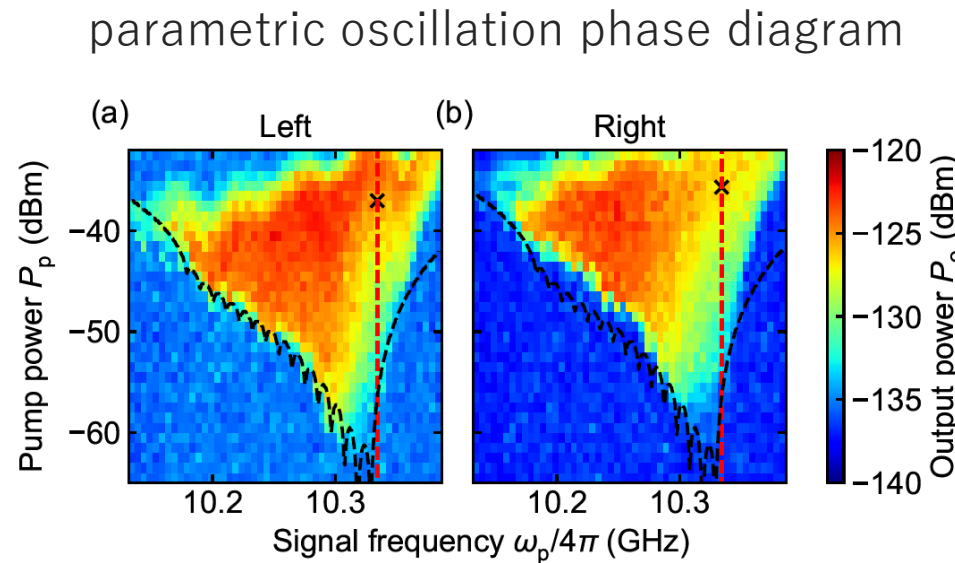
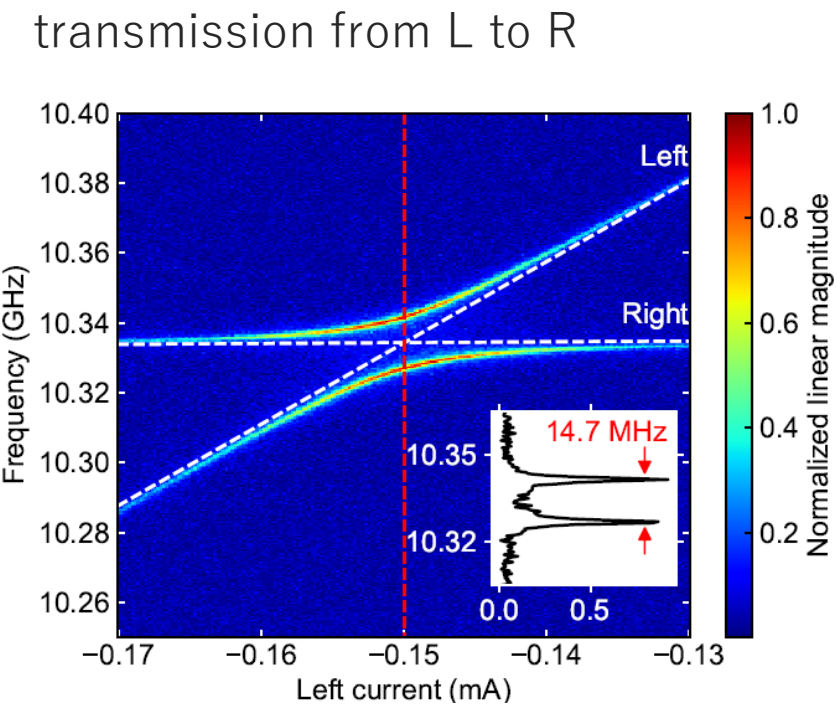


$$C_{\text{in}} : 3.4 \text{ fF } (Q_{\text{ext}} \sim 10^4)$$
$$C_c : 0.6 \text{ fF } (g \sim 7 \text{ MHz})$$
$$I_c : 1.0 \mu\text{A/JJ}$$

Coupling between KPO's

T. Yamaji *et al.*, arXiv:2212.13682.

- ◆ avoided level crossing due to coupling capacitance
- ◆ single-photon Kerr regime ($K_{L,R} \sim 10\kappa_{L,R}$)
- ◆ (independent) parametric oscillation phase diagram consistent with theory [1]



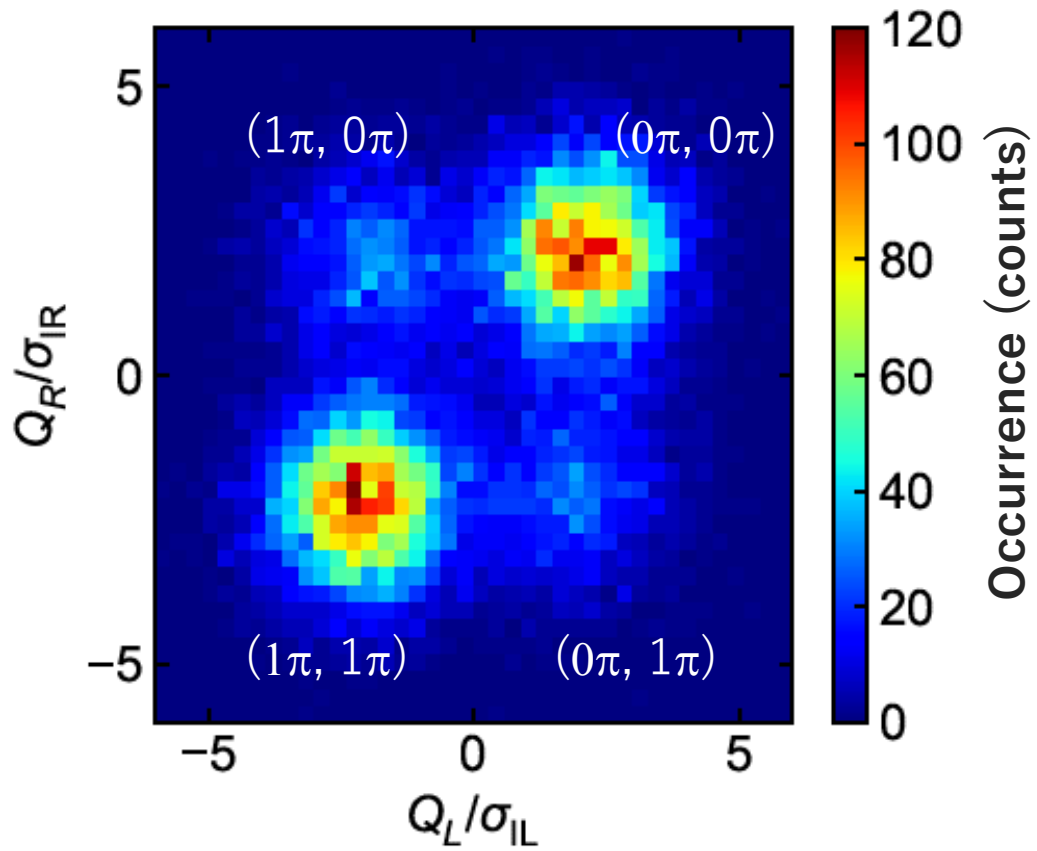
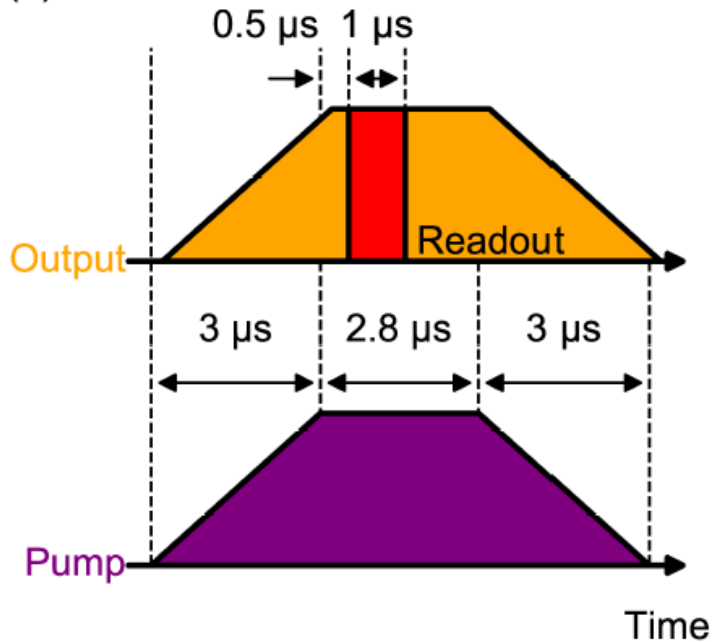
black line: theory $\langle a^+ a \rangle = 1$

[1] N. Bartolo et al., Phys. Rev. A **94**, 033841 (2016).

Correlated parametric oscillation

T. Yamaji *et al.*, arXiv:2212.13682.

- ◆ simultaneously apply pulsed pump and detect the output phase
- ◆ probability of the same phase is higher (ferromagnetic correlation)



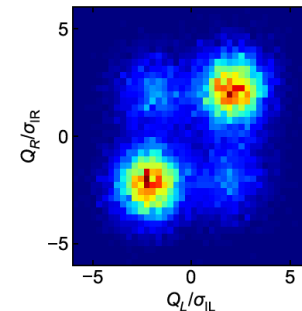
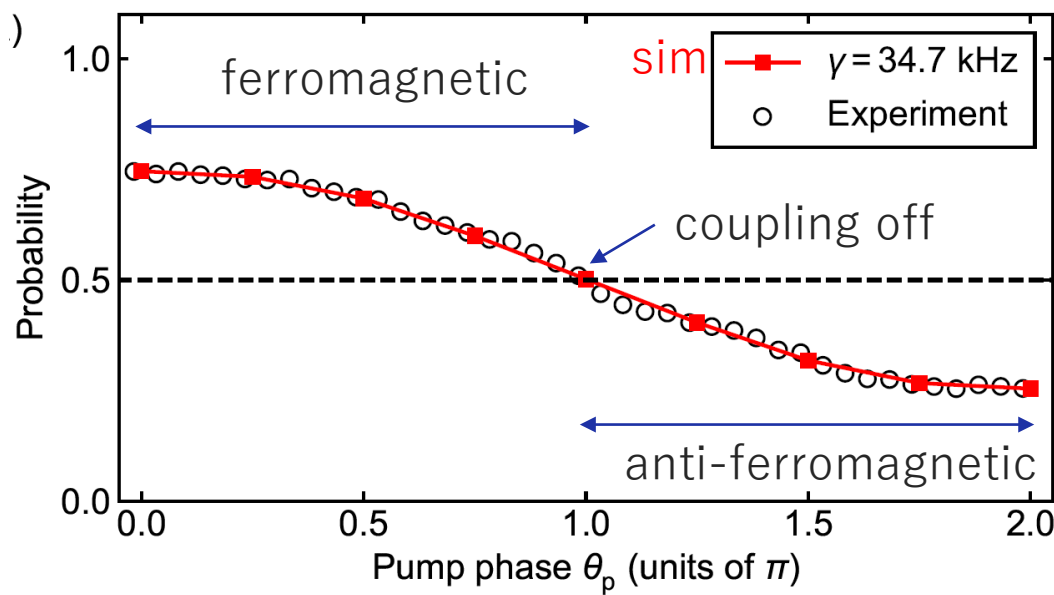
Controllable coupling with pump phase

S. Masuda et al., Phys. Rev. Appl. **18**, 034076 (2022).
T. Yamaji et al., arXiv:2212.13682.

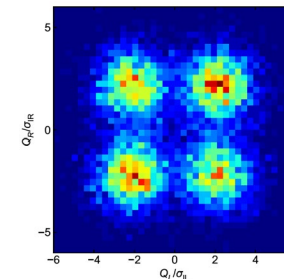
- ◆ Demonstration of controllable coupling by pump phase (**no on-chip control!**)
- ◆ Agree with numerical simulation by adjusting (unknown) dephasing rate

$$\mathcal{H}/\hbar = \sum_{i=L,R} \left[\frac{K_i}{2} a_i^{\dagger 2} a_i^2 + \Delta_i a_i^{\dagger} a_i + \frac{p_i}{2} (a_i^{\dagger 2} + a_i^2) \right] \\ + g \left(e^{-i\theta_p/2} a_L^\dagger a_R + e^{i\theta_p/2} a_L a_R^\dagger \right),$$

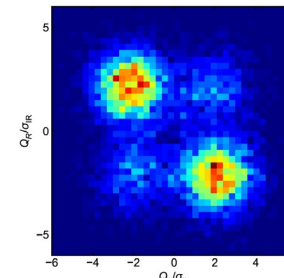
coupling term



$\theta_p/2=0$
ferromagnetic
coupling



$\theta_p/2=\pi/2$
coupling off



$\theta_p/2=\pi$
antiferromagn.
coupling

Summary

- ◆ Superconducting Kerr parametric oscillator
 - derived from Josephson parametric amplifier/oscillator
 - single-photon Kerr regime ($K \gg \kappa$)
- ◆ New paradigm for quantum information processing
 - Quantum annealing
 - quantum bifurcation machine
 - Fault-tolerant quantum computing
 - hardware efficient
 - biased noise qubit



This presentation is partly based on results obtained from a project, JPNP16007, commissioned by the New Energy and Industrial Technology Development Organization (NEDO).

\Orchestrating a brighter world

NEC creates the social values of safety, security, fairness and efficiency to promote a more sustainable world where everyone has the chance to reach their full potential.



\Orchestrating a brighter world

NEC